AIAA JOURNAL
Vol. 49, No. 3, March 2011

Novel Uncertainty Propagation Method for Robust Aerodynamic Design

Mattia Padulo*
Cranfield University, Cranfield, England MK43 0AL, United Kingdom
M. Sergio Campobasso†
University of Glasgow, Glasgow, Scotland G12 8QQ, United Kingdom
and
Marin D. Guenov‡
Cranfield University, Cranfield, England MK43 0AL, United Kingdom

DOI: 10.2514/1.J050448

Starting from a comparative study of various methods for uncertainty propagation, this paper presents a novel reduced quadrature technique to be used in gradient-based robust design optimization of aerodynamic shapes. The accuracy and computational efficiency of the method are investigated by means of mathematical analyses and numerical examples. The method is then applied to the robust design of airfoils under probabilistic uncertainty. It is shown that the solutions obtained through the proposed method can outperform those obtained through linearization, without any significant increase in computational cost.

Nomenclature

F	=	robust objective function
f	=	objective function
G_i	=	ith robust constraint function
g_i	=	ith constraint function
n	=	dimension of design space
$p_{\mathbf{y}}$	=	joint probability density function of multivariate random variable $\mathbf{y}$
$\mathbf{x}$	=	vector of design variables
Γ_y	=	kurtosis of random variable y
γ_y	=	skewness of random variable y
μ_y	=	expectation of random variable y
σ_y	=	standard deviation of random variable y

I. Introduction

MODERN aerodynamic design relies on the use of computational fluid dynamics (CFD) tools to predict the performance of the aerodynamic shape under consideration. Very promising designs can be obtained, in principle, by coupling the CFD code with an appropriate optimization algorithm. However, at the inception of the development process, the complete problem frame is usually only approximately known, the adopted computer models have low fidelity and assumptions based on previous experience have to be largely used. Because of such an uncertain basis, the aerodynamic shape may require several adjustments before the design is frozen. If the identified optimal solution is sufficiently sensitive to perturbations of the design variables, such adjustments may severely degrade the original design performance and would require rework or fixes. These observations highlight the usefulness of seeking the shape robustness against unforeseen changes, which is the main motivation behind our research and can be ascribed to the field of robust design optimization (RDO) [1]. The original RDO methodology is due to Taguchi, and it was based on direct experimentation, as documented by the English book on the subject by Phadke [2]. It was then extended to simulation-based design and gradually improved by using nonlinear constrained optimization techniques [3]. The constrained RDO strategy is made up of three main parts. The first stage consists of identifying, qualifying, and quantifying the sources of uncertainty associated with the design input and the analysis modules. This is usually done by means of stochastic models. The second phase consists of propagating the uncertainty through the analysis system to obtain a probabilistic description of the objective functions and constraints. Robust forms of objectives and constraints typically depend on expectation and variance of their deterministic counterparts. Finally, the third stage consists of optimizing the robust objectives subject to the robust constraints. The robust optimal design is such that the expectation of the objectives is optimized and their variances are minimized. This paper focuses on the second stage of RDO. Existing approaches to perform such a task, which include the Monte Carlo simulation (MCS), the Taylor-based method of moments (MM), the Gaussian quadrature (GQ), and stochastic expansion (SE), show significant drawbacks when applied to classical gradient-based shape optimization. Such difficulties are either due to the unsatisfactory accuracy of the propagation or to its excessive computational cost. This paper addresses these two issues: its main objective is to present a novel propagation technique, which exhibits a convenient tradeoff between the accuracy and the efficiency of mean and variance approximations and supplies robust objectives and constraints in a form that can be suitably handled by gradient-based optimizers. Such a technique may constitute an alternative to uncertainty analysis based on first-order derivatives, which has often been used in RDO due to its simplicity and computational speed. This is because the accuracy of the proposed method (as demonstrated later on in the paper) is higher than that of the moment propagation based on first-order derivatives in the case of nonlinear problems, while the computational cost of the two approaches is comparable.

The paper is structured as follows. The mathematical formulation of the RDO problem is outlined in Sec. II, along with a review of suitable uncertainty quantification approaches. The novel propagation method is reported in Sec. III. By employing a set of simple but meaningful analytical functions, the method is compared in Sec. IV to uncertainty propagation strategies based on linearization, higher-order expansions, and Stroud quadrature formulas [4–6]. The

Received 10 February 2010; revision received 19 November 2010; accepted for publication 23 November 2010.

*Ph.D. Student, School of Engineering; currently NASA Postdoctoral Program Fellow, NASA Glenn Research Center, Cleveland, Ohio 44135.
†Lecturer, School of Engineering.
‡Professor, School of Engineering. Senior Member AIAA (Corresponding Author).

application of the proposed technology in the framework of gradient-based RDO is examined in Sec. V, while in Sec. VI, the novel propagation approach is contrasted with linearization as applied to the problem of robust shape optimization of a transonic airfoil under geometric uncertainty. Conclusions are drawn in Sec. VII.

II. Background

Assume that the design analyses consist of evaluating the functions $f(\mathbf{x})$ and $g_i(\mathbf{x})$, $i = 1, 2, \ldots, I$, with $\mathbf{x} \in \mathbb{R}^n$. The deterministic design optimization problem can be formulated as follows:

Find

$$\mathbf{x} \in \mathbb{R}^n \tag{1}$$

to minimize

$$f(\mathbf{x})$$

subject to

$$g_i(\mathbf{x}) \leqslant 0; \qquad i = 1, 2, \ldots, I$$

and

$$\mathbf{x}_L \leqslant \mathbf{x} \leqslant \mathbf{x}_U$$

The identification and quantification of uncertainties affecting the input variables and/or parameters by means of probabilistic models renders problem (1) stochastic. The resulting design optimization problem under uncertainty can be written as follows:

Find

$$\boldsymbol{\mu}_{\mathbf{x}} \in \mathbb{R}^n \tag{2}$$

to minimize

$$\mu_f + k_f \sigma_f$$

subject to

$$\mu_{g_i} + k_{g_i} \sigma_{g_i} \leqslant 0; \quad i = 1, 2, \ldots, I$$

and

$$\mathbf{x}_L + k_{\mathbf{x}} \boldsymbol{\sigma}_{\mathbf{x}} \leqslant \boldsymbol{\mu}_{\mathbf{x}} \leqslant \mathbf{x}_U - k_{\mathbf{x}} \boldsymbol{\sigma}_{\mathbf{x}}$$

where k_f, k_{g_i}, and $k_{\mathbf{x}}$ are suitably chosen coefficients. If all variables are continuous, the mean and variance of $f(\mathbf{x})$ are given by

$$\mu_f = E[f(\mathbf{x})] = \int_{-\infty}^{+\infty} f(\mathbf{x}) p_{\mathbf{x}}(\mathbf{x})\, \mathrm{d}\mathbf{x} \tag{3}$$

$$\sigma_f^2 = E[(f(\mathbf{x}) - \mu_f)^2] = \int_{-\infty}^{+\infty} [f(\mathbf{x}) - \mu_f]^2 p_{\mathbf{x}}(\mathbf{x})\, \mathrm{d}\mathbf{x} \tag{4}$$

Unfortunately, a closed-form solution for these integrals does not, in general, exist for problems of practical interest. The numerical approximation of these statistical moments requires a tradeoff between computational cost and accuracy. Existing methods for performing such a task, also termed uncertainty propagation, include the Taylor-based MM, the GQ techniques, the MCS methods, and SE. Such methods are reviewed in the following subsections.

A. Taylor-Based Moment Propagation

When the system response is differentiable a sufficient number of times with respect to the uncertain variables $\mathbf{x}$, its statistical moments can be calculated through a Taylor-series expansion around $\boldsymbol{\mu}_{\mathbf{x}}$. The resulting method is also known as MM. Consider the Taylor-series expansion of f truncated to the fourth order:

$$\begin{aligned} f_{\mathrm{MM}} = {} & f(\boldsymbol{\mu}_{\mathbf{x}}) + \sum_{p=1}^{n} \left(\frac{\partial f}{\partial x_p}\right) \Delta x_p + \frac{1}{2} \sum_{p=1}^{n} \sum_{q=1}^{n} \left(\frac{\partial^2 f}{\partial x_p \partial x_q}\right) \Delta x_p \Delta x_q \\ & + \frac{1}{6} \sum_{p=1}^{n} \sum_{q=1}^{n} \sum_{r=1}^{n} \left(\frac{\partial^3 f}{\partial x_p \partial x_q \partial x_r}\right) \Delta x_p \Delta x_q \Delta x_r \\ & + \frac{1}{24} \sum_{p=1}^{n} \sum_{q=1}^{n} \sum_{r=1}^{n} \sum_{s=1}^{n} \left(\frac{\partial^4 f}{\partial x_p \partial x_q \partial x_r \partial x_s}\right) \Delta x_p \Delta x_q \Delta x_r \Delta x_s \\ & + O(\Delta \mathbf{x}^5) \end{aligned} \tag{5}$$

in which $\Delta x_p = x_p - \mu_{x_p}$ and the partial derivatives of f with respect to the input variables are computed at $\mathbf{x} = \boldsymbol{\mu}_{\mathbf{x}}$. The term $O(\Delta \mathbf{x}^5)$ denotes the remainder; that is, all terms of order five and higher. In the case of independent input variables, the following expressions can be obtained for mean and variance:

$$\begin{aligned} \mu_{f_{\mathrm{MM}}} = \int_{-\infty}^{+\infty} f_{\mathrm{MM}} p_{\mathbf{x}}\, \mathrm{d}\mathbf{x} = {} & \overbrace{f(\boldsymbol{\mu}_{\mathbf{x}})}^{M_1} + \overbrace{\frac{1}{2} \sum_{p=1}^{n} \left(\frac{\partial^2 f}{\partial x_p^2}\right) \sigma_{x_p}^2}^{M_2} \\ & + \overbrace{\frac{1}{6} \sum_{p=1}^{n} \left(\frac{\partial^3 f}{\partial x_p^3}\right) \gamma_{x_p} \sigma_{x_p}^3}^{M_3} + \overbrace{\frac{1}{24} \sum_{p=1}^{n} \left(\frac{\partial^4 f}{\partial x_p^4}\right) \Gamma_{x_p} \sigma_{x_p}^4}^{M_4} \\ & + \overbrace{\frac{1}{8} \sum_{p=1}^{n} \sum_{\substack{q=1 \\ q \neq p}}^{n} \left(\frac{\partial^4 f}{\partial x_p^2 \partial x_q^2}\right) \sigma_{x_p}^2 \sigma_{x_q}^2}^{M_5} + O(\boldsymbol{\sigma}_{\mathbf{x}}^5) \end{aligned} \tag{6}$$

$$\begin{aligned} \sigma_{f_{\mathrm{MM}}}^2 = \int_{-\infty}^{+\infty} (f_{\mathrm{MM}} - \mu_{f_{\mathrm{MM}}})^2 p_{\mathbf{x}}\, \mathrm{d}\mathbf{x} = {} & \overbrace{\sum_{p=1}^{n} \left(\frac{\partial f}{\partial x_p}\right) \sigma_{x_p}^2}^{V_1} \\ & + \overbrace{\sum_{p=1}^{n} \left(\frac{\partial^2 f}{\partial x_p^2}\right) \left(\frac{\partial f}{\partial x_p}\right) \gamma_{x_p} \sigma_{x_p}^3}^{V_2} + \overbrace{\sum_{p=1}^{n} \sum_{\substack{q=1 \\ q \neq p}}^{n} \left(\frac{\partial^3 f}{\partial x_p^2 \partial x_q}\right) \left(\frac{\partial f}{\partial x_q}\right) \sigma_{x_p}^2 \sigma_{x_q}^2}^{V_3} \\ & + \overbrace{\frac{1}{2} \sum_{p=1}^{n} \sum_{\substack{q=1 \\ q \neq p}}^{n} \left(\frac{\partial^2 f}{\partial x_p \partial x_q}\right)^2 \sigma_{x_p}^2 \sigma_{x_q}^2}^{V_4} + \overbrace{\frac{1}{3} \sum_{p=1}^{n} \left(\frac{\partial^3 f}{\partial x_p^3}\right) \left(\frac{\partial f}{\partial x_p}\right) \Gamma_{x_p} \sigma_{x_p}^4}^{V_5} \\ & + \overbrace{\frac{1}{4} \sum_{p=1}^{n} \left(\frac{\partial^2 f}{\partial x_p^2}\right)^2 (\Gamma_{x_p} - 1) \sigma_{x_p}^4}^{V_6} + O(\boldsymbol{\sigma}_{\mathbf{x}}^5) \end{aligned} \tag{7}$$

where the term $O(\boldsymbol{\sigma}_{\mathbf{x}}^5)$ denotes all monomials of order five or higher: namely, terms proportional to $\sigma_{x_p}^5$, $\sigma_{x_p}^3 \sigma_{x_q}^2$, $\sigma_{x_p}^3 \sigma_{x_q}^3$, etc. As in Eq. (5), the partial derivatives of f with respect to the input variables are computed at $\mathbf{x} = \boldsymbol{\mu}_{\mathbf{x}}$. The skewness γ_{x_p} and the kurtosis Γ_{x_p} for variable x_p are defined as follows:

$$\gamma_{x_p} = \frac{E[(x_p - \mu_{x_p})^3]}{\sigma_{x_p}^3} \tag{8}$$

$$\Gamma_{x_p} = \frac{E[(x_p - \mu_{x_p})^4]}{\sigma_{x_p}^4} \tag{9}$$

Hereafter, a Roman number will indicate the truncation order of the method: e.g., I MM will denote first-order MM, and so on. I MM is often used in literature [7–10]. However, even for relatively small spread of the input variables, the accuracy of the method may be severely spoiled by nonlinearities in the system response. One way of improving this method would be to consider higher-order Taylor-series expansions: for example, retaining second-order terms [8,11,12]. The downside associated with this strategy is that, while

the second-order terms guarantee a better accuracy of the approximation to the mean by retaining the term M_2 in Eq. (6), this is not necessarily the case for the approximation to the variance. Consider Eq. (7) in the case of symmetric input variables, for which the term V_2 is zero. The estimation of the variance of order $\boldsymbol{\sigma}_{\mathbf{x}}^4$, required to improve the accuracy with respect to the linearization, is obtained by retaining not only the terms V_4 and V_6 but also the terms V_3 and V_5. However, this would require the calculation of the third derivatives contained in V_3 and V_5. The principal advantage of this method is a great computational efficiency, to a degree that depends on the available methods for calculating derivatives. In particular, it benefits from techniques such as automatic differentiation (AD) [13–16], which allows one to obtain, at a low computational cost, derivatives that are exact to machine accuracy or the complex variable method (CVM) [17].

B. Gaussian Quadrature

GQ formulas give the approximation of the integral of a function $f(\mathbf{x})$ on a domain $D \subset \mathbb{R}^n$ by a properly weighted sum of particular values $f(\mathbf{x}_i)$, $i = 1, \ldots N$, where the $\mathbf{x}_i$ are N suitably selected points in D, also called nodes. For the case of scalar x, such formulas require the fewest evaluations to obtain a given degree of accuracy, and they are largely used in practice. The straightforward approach to multivariate integration is called a product rule, which consists of applying such formulas to each of the n dimensions of D. More precisely, assume that $D = D_1 \times D_2 \times \ldots \times D_n$, where $\times$ denotes the Cartesian product, and $D_i \subset \mathbb{R}$, for $i = 1, \ldots, n$. If we apply the same one-dimensional integration rule with N nodes and given weights W_i to each D_i, the integrals in Eqs. (3) and (4) can be approximated as follows:

$$\mu_{f_{\mathrm{GQ}}} = \sum_{i1}^{N} W_{i1} \left\{ \sum_{i2}^{N} W_{i2} \left[\ldots \sum_{\mathrm{in}}^{N} W_{\mathrm{in}} f(\mathbf{x}_{i1,i2,\ldots,\mathrm{in}}) \right] \right\} \tag{10}$$

$$\sigma_{f_{\mathrm{GQ}}}^2 = \sum_{i1}^{N} W_{i1} \left(\sum_{i2}^{N} W_{i2} \left\{ \ldots \sum_{\mathrm{in}}^{N} W_{\mathrm{in}} [f(\mathbf{x}_{i1,i2,\ldots,\mathrm{in}}) - \mu_{f_{\mathrm{GQ}}}]^2 \right\} \right) \tag{11}$$

Three-node formulas ($N = 3$) are usually adopted to obtain a sufficient accuracy. The arrays of design variables in Eqs. (10) and (11) are distributed at the vertices of an hypergrid of dimension 3^n. The vector associated with $i1 = i2 = \cdots = in = 2$ corresponds to the mean of the input variables $\boldsymbol{\mu}_{\mathbf{x}}$. Denoting suitable scalars by h^+ and h^-, the states with one or more subscript ip equal to one have the corresponding components perturbed by $h^- \sigma_{x_{ip}}$ with respect to their mean, whereas the states with one or more subscript ip equal to three have the corresponding components perturbed by $h^+ \sigma_{x_{ip}}$. Three values for weights W_i and the values for h^+ and h^- then have to be determined.

In the field of statistical tolerance design, for the case of independent Gaussian variables, Taguchi [18] proposed a solution for which equal weights $W_i = \frac{1}{3}$, and $h^+ = -h^- = h_{\mathrm{GQ}} = \frac{\sqrt{3}}{2}$ were used. D'Errico and Zaino [19] modified this approach, suggesting the adoption of $h_{\mathrm{GQ}} = \sqrt{3}$ and distinct weights $W_i = \{\frac{1}{6}, \frac{2}{3}, \frac{1}{6}\}$. Seo and Kwak [20] generalized this approach to consider non-Gaussian distributions. However, methods adopting full factorial designs, despite attaining an accuracy of $O(\boldsymbol{\sigma}_{\mathbf{x}}^5)$, have limited application in computational robust design [21], since the number of function evaluations required is 3^n. Evans [22] proposed an improved integration technique for which the approximated mean and variance can be obtained from the weighted sum of $2n^2 + 1$ function evaluations, corresponding to suitable sampling points in the input space. Evans also showed that the error of his formula is $O(\boldsymbol{\sigma}_{\mathbf{x}}^5)$ in the general case and $O(\boldsymbol{\sigma}_{\mathbf{x}}^6)$ in the case where all the input distributions are symmetric. Other similar techniques, known by the name of sigma-point (SP) methods [23–26], were developed for control systems applications. They require $2n + 1$ function evaluations and exhibit an error of $O(\boldsymbol{\sigma}_{\mathbf{x}}^3)$ in the general case and $O(\boldsymbol{\sigma}_{\mathbf{x}}^4)$ in the case where all the input distributions are symmetric. A general framework for reduced-order quadrature formulas is provided by the generalized dimension-reduction method [27], which can be considered as embracing both Evans method [22] and SP methods as bivariate and univariate formulas, respectively. In particular, the univariate method [28] has received special attention in recent literature [29–33]. Quadrature formulas requiring $n + 1$ and $2n$ function evaluations were introduced by Stroud [4,5] to exactly integrate polynomials of order two and three, respectively, and extended to calculate expectation integrals by Xiu [6], who gave weights and nodes for various symmetric and asymmetric distributions. Their accuracy is $O(\boldsymbol{\sigma}_{\mathbf{x}}^2)$ for both mean and variance estimations.

C. Monte Carlo Methods

Several techniques, collected here under the name of the MCS methods, originate from the stochastic interpretation of the integrals in Eqs. (3) and (4). Probability distributions over the outputs of a process induced by the probability distribution over the inputs are obtained by performing m repetitions of the process, each of which corresponds to a sampling point $\mathbf{x}_i$ drawn from the input space. For the simplest case of random sampling, unbiased estimators for the integrals in Eqs. (3) and (4) are given by the following formulas:

$$\mu_{f_{\mathrm{MCS}}} = \frac{1}{m} \sum_{i=1}^{m} f(\mathbf{x}_i) \tag{12}$$

$$\sigma_{f_{\mathrm{MCS}}}^2 = \frac{1}{m-1} \sum_{i=1}^{m} [f(\mathbf{x}_i) - \mu_{f_{\mathrm{MCS}}}]^2 \tag{13}$$

Both $\mu_{f_{\mathrm{MCS}}}$ and $\sigma_{f_{\mathrm{MCS}}}^2$ converge to their expected value with an error that is $O(m^{-(1/2)})$; thus, the number of required runs depends on the desired relative accuracy for the output distribution, but it is independent of the number of inputs n. Variance reduction techniques [34], such as control variates, antithetic variables, importance, stratified, Latin hypercube [35], and descriptive sampling [36], have been developed to achieve faster convergence for MCS methods. An improved rate of convergence can be obtained, for problems with low to medium dimensionality, by also using the so-called quasi-Monte Carlo methods, which substitute computer-generated pseudorandom numbers with low-discrepancy sequences [37]. MCS methods are a simple and robust solution for multidimensional integration. However, the number of function evaluations required suggests adoption of, if possible, alternative methods for RDO, particularly in the case of computationally demanding analysis codes. Finally, MCS approaches require appropriate optimization algorithms able to handle the noise introduced by the propagation phase in the robust objective and constraint functions [38], such as evolutionary algorithms [39,40], stochastic approximation [41–43], and generating set search methods [44]. By contrast, Taylor-based MM and GQ supply noise-free robust objectives and constraints, which can be handled by classical gradient-based deterministic optimization methods [45].

D. Stochastic Expansion

Polynomial chaos expansion (PCE) [46] and stochastic collocation (SC) [47] are two related techniques that expand f in a series of random variables, hence the name of SE. Given such expansion, the required moments can be calculated analytically. PCE and SC were originally developed to solve stochastic partial differential equations. Here, the focus is on the so-called nonintrusive versions of these methods, which consider the deterministic function f as a black box. Supposing that f is square integrable, its PCE can be written as

$$f = a_0 H_0 + \sum_{i1=1}^{\infty} a_{i1} H_1(u_{i1}) + \sum_{i1=1}^{\infty} \sum_{i2=1}^{i1} a_{i1,i2} H_2(u_{i1}, u_{i1}) + \sum_{i1=1}^{\infty} \sum_{i2=1}^{i1} \sum_{i3=1}^{i2} a_{i1,i2,i3} H_3(u_{i1}, u_{i2}, u_{i3}) + \cdots \tag{14}$$

where $\mathbf{u}$ is a vector of standard normal variables (which can be derived from $\mathbf{x}$ by resorting to the Rosenblatt transformation [48]), H_q is a qth-order multidimensional Hermite polynomial, and the a_i are suitable coefficients. The expansion can also be performed as a function of other kinds of random variables (also of mixed type) if other suitable polynomials belonging to the Askey scheme are chosen instead of the Hermite polynomials [49]. For example, Legendre, Jacobi, and Laguerre polynomials correspond to uniform, beta, and exponential distribution, respectively. If we truncate the expansion at the order N_t, we can adopt the following shortened notation:

$$f \approx \sum_{q=0}^{N_t} b_q \chi_q(\mathbf{u}) \tag{15}$$

where b_q corresponds to $a_{i1,i2,\ldots,in}$, and χ_q corresponds to $H_n(u_{i1}, u_{i2}, \ldots, u_{in})$. There are several ways to obtain the coefficients b_q. For example, by projecting the response f against the basis function χ_q, the so-called spectral projection can be performed:

$$b_q = \frac{E[f\chi_q(\mathbf{u})]}{E[\chi_q^2(\mathbf{u})]} \tag{16}$$

where the denominator can be calculated analytically, and the numerator can be calculated by any quadrature technique, including MCS and GQ. The coefficients can also be found by linear regression over the vector of responses $\mathbf{f}$, which is obtained as a result of a design of experiments:

$$\boldsymbol{\chi}_q \mathbf{b} = \mathbf{f} \tag{17}$$

In a similar way to PCE, SC writes f as

$$f \approx \sum_{q=0}^{N_t} L_q(\mathbf{x}) f(\mathbf{x}_q) \tag{18}$$

where $L_q(\mathbf{x})$ derives from the application of the tensor-product rule [50] to the one-dimensional Lagrange interpolation polynomial, given by the following expression:

$$L_q(x) = \prod_{\substack{p=1 \\ p \neq q}}^{N} \frac{x - x_p}{x_q - x_p} \tag{19}$$

The optimal choice of $\mathbf{x}_q$ is that associated with the so-called Gauss points: i.e., the roots of the orthogonal polynomial belonging to the Askey scheme. Hence, the major difference between PCE and SC is that PCE has to find the coefficients b_q, given that a polynomial basis is known, whereas SC gets the coefficients from functional values corresponding to the Gauss points and has to determine an interpolant polynomial [50]. It is found in practice that, if the same set of collocation points is considered, SC can require fewer function evaluations than PCE to achieve the desired accuracy. However, SC is less flexible than PCE, which can also evaluate the function of interest at points that do not belong to the set of Gauss points, thus increasing the simulation fault tolerance [50]. The interest in SE methods for design applications is quite recent [31,51,52]. However, when only the first moments are of interest, there is no clear advantage in employing SE instead of GQ techniques [31]. On the other hand, when randomization is involved in the determination of the coefficients, the same difficulties already discussed for MCS would hinder the application of gradient-based methods to the RDO problem.

III. Proposed Uncertainty Propagation Method

The proposed propagation method is based on a quadrature approach that we may term univariate reduced quadrature (URQ) to be consistent with the nomenclature introduced in [28]. Starting from the SP methods [25] and Evans's statistical tolerancing method [22], with the aim of obtaining an univariate integration method for generic nonsymmetric distributions, the following formulas to estimate mean and variance are obtained (also see the Appendix):

$$\mu_{f_{\mathrm{URQ}}} = W_0 f(\boldsymbol{\mu}_{\mathbf{x}}) + \sum_{p=1}^{n} W_p \left[\frac{f(\mathbf{x}_p^+)}{h_p^+} - \frac{f(\mathbf{x}_p^-)}{h_p^-} \right] \tag{20}$$

$$\sigma^2_{f_{\mathrm{URQ}}} = \sum_{p=1}^{n} \left\{ W_p^+ \left[\frac{f(\mathbf{x}_p^+) - f(\boldsymbol{\mu}_{\mathbf{x}})}{h_p^+} \right]^2 + W_p^- \left[\frac{f(\mathbf{x}_p^-) - f(\boldsymbol{\mu}_{\mathbf{x}})}{h_p^-} \right]^2 + W_p^{\pm} \frac{[f(\mathbf{x}_p^+) - f(\boldsymbol{\mu}_{\mathbf{x}})][f(\mathbf{x}_p^-) - f(\boldsymbol{\mu}_{\mathbf{x}})]}{h_p^+ h_p^-} \right\} \tag{21}$$

The sampling points are found as follows:

$$\mathbf{x}_p^{\pm} = \boldsymbol{\mu}_{\mathbf{x}} + h_p^{\pm} \sigma_{x_p} \mathbf{e}_p \tag{22}$$

where $\mathbf{e}_p$ is the pth vector of the identity matrix of size n and $h_p^{\pm}$ are given by

$$h_p^{\pm} = \frac{\gamma_{x_p}}{2} \pm \sqrt{\Gamma_{x_p} - \frac{3\gamma_{x_p}^2}{4}} \tag{23}$$

It can be demonstrated [53] that the quantities $h_p^{\pm}$ defined in Eq. (23) are always real numbers for our cases of interest (i.e., input distributions having finite first four moments). The weights have to be chosen as

$$W_0 = 1 + \sum_{p=1}^{n} \frac{1}{h_p^+ h_p^-}; \qquad W_p = \frac{1}{h_p^+ - h_p^-}$$

$$W_p^+ = \frac{(h_p^+)^2 - h_p^+ h_p^- - 1}{(h_p^+ - h_p^-)^2}; \qquad W_p^- = \frac{(h_p^-)^2 - h_p^+ h_p^- - 1}{(h_p^+ - h_p^-)^2}$$

$$W_p^{\pm} = \frac{2}{(h_p^+ - h_p^-)^2}$$

The proposed method requires $2n + 1$ function evaluations. Hence, its cost is comparable to the linearization method: namely, the moment propagation method in which the first-order derivatives are determined by means of finite differences. As discussed in Sec. III.B, however, the accuracy of URQ is higher than that associated with the linearization method.

A. Requirements of Input Variables

The quantification of input uncertainties is usually performed before the design optimization process. The mathematical model is chosen to match, as closely as possible, the uncertain knowledge about the design problem being considered, which is either based on sufficiently significant statistical data or relies on expert opinion, or a combination of both. It is well known that a correct quantification of the input uncertainty is paramount for the reliability of the optimization. In principle, the more information one can include into the input probabilistic model, the better, as long as the type and level of uncertainty data are necessary and/or sufficient for the chosen design strategy and can be handled by the adopted propagation technique. For example, a detailed modeling of input distribution tails is usually of secondary importance in RDO, which focuses on variations around the mean. Similarly, a popular propagation method, such as first-order Taylor-based MM, would make no use of more information than the first two moments of the input variables. A key requirement of the presented propagation approach is that the first four moments be available for each uncertain variable. Typically, such information is available in three circumstances:

1) For independent input variables, the input marginal distributions, each identifying weights and nodes for the quadrature rule, are known. The joint probability density function (PDF) is, in this case, given as the product of all the marginal PDFs.

2) For correlated input variables, if the marginal distributions (which do not have to be identical) are known, it is always possible to transform the original set of variables into an uncorrelated set of variables. For example, this can be achieved by means of the spectral decomposition [54]

$$\Sigma_{xx} = VDV^{-1} \tag{24}$$

where

$$\Sigma_{xx} = \begin{bmatrix} \sigma_{x_1}^2 & \rho_{1,2}\sigma_{x_1}\sigma_{x_2} & \cdots & \rho_{1,n}\sigma_{x_1}\sigma_{x_n} \\ \rho_{1,2}\sigma_{x_1}\sigma_{x_2} & \sigma_{x_2}^2 & \cdots & \rho_{2,n}\sigma_{x_2}\sigma_{x_n} \\ \vdots & \vdots & \ddots & \vdots \\ \rho_{n,1}\sigma_{x_n}\sigma_{x_1} & \rho_{n,2}\sigma_{x_n}\sigma_{x_2} & \cdots & \sigma_{x_n}^2 \end{bmatrix}$$

is the input covariance matrix, and $\rho_{i,j} = [\mathrm{cov}(x_i, x_i)]/\sigma_{x_i}\sigma_{x_j}$ is the Pearson product-moment correlation coefficient;

V is the matrix of the right eigenvectors of Σ_{xx}, giving the principal axis of the input distribution, and hence the new coordinate system $\mathbf{x}'$;

D is the diagonal matrix of the eigenvalues of Σ_{xx}, with each eigenvalue $\lambda_{ii} = \sigma_{x_i'}^2$.

The interesting feature of such decomposition is that it allows correlation to be included in a straightforward way into the propagation phase by choosing the new points as

$$\mathbf{x}_p^{\pm} = \boldsymbol{\mu}_{\mathbf{x}} + Ch_p^{\pm}\mathbf{e}_p \tag{25}$$

where $C = V\sqrt{D}$. Geometrically, this corresponds to a rotation of the input variable sampling stencil. The spectral decomposition can be applied to a larger class of distributions than the multivariate Gaussian distribution. In this particular case, the computationally cheaper Cholesky decomposition [54] may be adopted, which gives the covariance matrix as $\Sigma_{xx} = CC^T$, where C^T is a lower triangular matrix.

3) For the known joint distribution, except for the textbook example of multivariate normal distribution, this case is quite rare. Should it be encountered, copulas [55,56] could be adopted to model the dependence between the variables. We would then resort to a Rosenblatt transformation [48] to reduce the input space to a standard Gaussian space and then perform the propagation.

B. Error Analysis for Generic Distributions

The accuracy of the first two statistical moments obtained by using the proposed URQ approach is assessed by means of fourth-order Taylor-series expansions. The first step consists of expanding $f(x_p^{\pm})$, appearing in Eqs. (20) and (21), about $\boldsymbol{\mu}_{\mathbf{x}}$, and inserting such expansions into the same equations. By doing so, one obtains the URQ approximation to the mean and variance of the output function f in terms of the moments of the input variables and the derivatives of f. We then define and calculate the error ε_{μ_f} of the URQ expectation of f as the difference between the expectation based on the fourth-order Taylor-series expansion [Eq. (6)] and the URQ expectation. Similarly, we define and calculate the error $\varepsilon_{\sigma_f^2}$ of the URQ variance of f as the difference between the variance based on the fourth-order Taylor-series expansion [Eq. (7)] and the URQ variance. The expressions of $\varepsilon_{\sigma_f^2}$ and $\varepsilon_{\sigma_f^2}$ are, respectively (see the Appendix for more details),

$$\varepsilon_{\mu_f} = M_5 + \text{terms of order} > \boldsymbol{\sigma}_{\mathbf{x}}^4 \tag{26}$$

$$\varepsilon_{\sigma_f}^2 = V_3 + V_4 + \text{terms of order} > \boldsymbol{\sigma}_{\mathbf{x}}^4 \tag{27}$$

These errors coincide with those obtained for one of the SP methods, the divided difference filter (DDF) [57], in the symmetric case [25], but they are smaller in the general, nonsymmetric case, since the DDF method cannot model the term $V_2 \propto \boldsymbol{\sigma}_{\mathbf{x}}^3$. Let us now compare the errors provided by Eqs. (26) and (27) with their counterparts when using I MM. Equation (6) shows that the latter method considers only the terms M_1 in the mean estimate, and Eq. (7) highlights that only the term V_1 is retained in the variance estimate. The proposed uncertainty propagation method yields an estimate of the mean, which is always more accurate than that obtained with I MM. This is because the mean predicted by the latter method is merely the output function evaluated at the mean of the input variables and thus appears, albeit incorrectly, as independent of the variance of the input variables. Conversely, the URQ mean has accuracy $O(\boldsymbol{\sigma}_{\mathbf{x}}^2)$, as it captures the contribution of the second derivative appearing in Eq. (6). In the case of nonsymmetric uncertainty distribution of the input variables, the accuracy of the URQ mean becomes even higher: namely, $O(\boldsymbol{\sigma}_{\mathbf{x}}^3)$ due to the resolved contribution of the third-order derivative appearing in Eq. (6).

When the uncertainty affecting the input variables is described by symmetric distributions ($\boldsymbol{\gamma}_{\mathbf{x}} = \mathbf{0}$) and the output function features significant cross dependencies of the input variables, the accuracy of the URQ variance estimate is $O(\boldsymbol{\sigma}_{\mathbf{x}}^2)$, which is comparable to that associated with the linearization method. In the case of nonsymmetrically distributed uncertainty of the inputs, however, the URQ variance becomes $O(\boldsymbol{\sigma}_{\mathbf{x}}^3)$, which is higher than that obtained with the linearization-based uncertainty propagation.

IV. Analytical Examples

The properties of the presented algorithms are now verified, assessed, and cross compared by analyzing the probabilistic response to uncertain input data of some simple but meaningful analytic functions, which are

1)

$$f(\mathbf{x}) = \sin(x_1 - 0.2)\sin(x_2 - 0.2)$$

2)

$$f(\mathbf{x}) = 0.5x_1^2 - 1.5x_1 + 0.7x_2^2 - 1.2x_2 + 1$$

3)

$$f(\mathbf{x}) = x_1^2 - 0.5x_1 + 2x_2^2 - 0.5x_2 + 0.5x_1^2x_2 + 0.05x_1^2x_2^2 + 0.3$$

4)

$$f(\mathbf{x}) = 1.7x_1^3 + (1.3 + 0.4x_2)x_1^2 + (0.8 - 2x_2^2)x_1 + 0.1x_2 - 2.8x_2^2 - 0.5x_2^3$$

These functions and their coefficients are expressly chosen to represent instances of output functions in which the terms M_2 to M_5 in Eq. (6) and V_2 to V_6 in Eq. (7) have different relative magnitudes. Such choice is performed on the basis of the error analysis carried out in the preceding section, and it aims to highlight the potential advantages and disadvantages of the proposed propagation method. For example, it is expected that the accuracy of the URQ variance will be higher for function 2 than for function 4, since the leading terms of the error in Eq. (27) are zero in the case of function 2 but not in the case of function 4. For the given four functions, URQ is compared with I MM, II MM, III MM, and when possible, with Stroud quadrature formulas. The last approach is available in two variants: one that integrates exactly polynomials of degree 2, and another that integrates exactly polynomials of degree 3. In the rest of this paper, the former variant is named S2, and the latter is named S3. The cross comparison of the probabilistic output of URQ, I MM, S2, and S3 is of particular interest, as it enables one to verify the expected higher accuracy of URQ with respect to methods of comparable cost: i.e., methods that require a number of function evaluations proportional to the number of uncertain variables. The II MM and III MM approaches are computationally more demanding than the four aforementioned methods, and they would be commonly deemed as computationally too expensive for engineering RDO. This is because, in the case $n \geq 2$, they require, respectively, $O(n^2)$ and $O(n^3)$ deterministic function evaluations for a single robust functional estimation, if finite differences are used. The analyses presented in this section, however, have been performed using the

Table 1 Number of function evaluations required by the propagation methods assessed in Sec. IV

Propagation method	Required function evaluations
I MM (FD)	$2n + 1$
II MM (FD)	$2n^2 + 1$
III MM (FD)	$2(n^2 + n) + 1$
S2	$n + 1$
S3	$2n$
URQ	$2n + 1$

analytical expression of the derivatives of the four functions. This type of analytical expression is generally not available in engineering design problems, whereby the derivatives required by the moment methods can be determined only by finite differencing in most cases. Therefore, a meaningful comparison of the computational burden associated with all the methods for uncertainty propagation presented in this paper has to be made by assuming the use of finite differencing for the moment methods. The number of function evaluations required by all uncertainty propagation methods under consideration for the calculation of mean and variance of the four selected functions is reported in Table 1. The number of function evaluations required by the three moment methods refers to the case in which second-order-accurate finite differences are used. It should be noted that, for the more general case of $n > 2$, the number of function evaluations required by the I and II MMs remains $O(n)$ and $O(n^2)$, respectively, but the number required by the III MM becomes $O(n^3)$. The respective costs of all other methods remain as those reported in Table 1 for any value of n. Despite the fact that II and III MMs are not frequently used in RDO due to their high computational cost, we include them in the comparative analysis provided next because these two methods allow one to better explain the Taylor-series-based estimation of the error associated with a particular quadrature formula. All derivatives required to obtain the results provided next have been calculated analytically. The results shown in Tables 2–7 are presented as percentage errors calculated with respect to the solution of a MCS with 5×10^7 samples. The mean of the input variables is fixed at $\boldsymbol{\mu}_{\mathbf{x}} = \mathbf{1}$. The accuracy of the considered methods is tested by gradually increasing the input standard deviation. Tables 2 and 3 provide, respectively, the mean and variance estimation corresponding to bivariate normal input variables, while Tables 4 and 5 report the same estimates for the case of uniform distribution of the input variables. Tables 6 and 7 deal instead with an instance of nonsymmetric input variables, the uncertainty of which has been modeled by generalized gamma distributions with skewness $\boldsymbol{\gamma}_{\mathbf{x}} = \mathbf{0.5}$ and unitary mean. As for the estimation of the mean, URQ approximates the function behavior better than I MM: for all three types of input uncertainty, the URQ error relative to the MCS result is at least one order of magnitude smaller (more than two orders in numerous instances) than the relative error observed when using I MM. The results of Table 6 reveal that, in the asymmetric case, the URQ relative error can be even smaller than that associated with II MM, which uses second-order derivatives. This is due to the fact that the URQ quadrature takes into account the term M_3 in Eq. (6), which includes third derivatives. In the symmetric cases, in which II MM and III MM coincide, S2, S3, and URQ exhibit a similar mean estimation accuracy. In the case of asymmetric input distributions, however, S2 shows a lower accuracy of the predicted mean with respect to URQ. This is due to the fact that, unlike URQ, S2 cannot model the term M_3 in Eq. (6). It should also be noted that it is not possible to apply S3 in the asymmetric case [6].

As for the estimation of the variance, in the symmetric case, URQ has the same accuracy of I MM, S2, and S3. The case of function 2 is an exception for which URQ performs better, since $f(\mathbf{x})$ does not have cross-derivative terms [the terms V_3 and V_4 in Eq. (7) are both zero]. If such terms are present but negligible, the URQ estimates approach the results of III MM. In such cases, URQ is more accurate than II MM for variance estimations. The opposite would be

Table 2 Mean estimation for Gaussian bivariate input distribution expressed as percentage error with respect to the solution of a MCS with 5×10^7 samples

Case	$\sigma_{\mathbf{x}}$	I MM	II MM III MM	S2	S3	URQ
1	0.05	0.250	0.007	0.003	−0.000	−0.000
	0.175	3.112	0.044	0.104	−0.030	−0.022
	0.3	9.408	−0.159	0.442	−0.292	−0.219
2	0.05	0.604	0.000	0.000	0.000	0.000
	0.175	7.926	−0.006	−0.006	−0.006	−0.006
	0.3	27.556	0.004	0.004	0.004	0.004
3	0.05	−0.315	−0.001	−0.001	−0.001	−0.001
	0.175	−3.732	−0.008	−0.020	−0.008	−0.008
	0.3	−10.227	−0.021	−0.075	−0.021	−0.021
4	0.05	0.044	−0.000	−0.002	−0.000	−0.000
	0.175	0.553	0.002	−0.049	0.002	0.002
	0.3	1.634	−0.002	−0.264	−0.002	−0.002

Table 4 Mean estimation for uniform bivariate input distribution expressed as percentage error with respect to the solution of a MCS with 5×10^7 samples

Case	$\sigma_{\mathbf{x}}$	I MM	II MM III MM	S2	S3	URQ
1	0.05	0.251	0.008	0.004	0.001	0.001
	0.175	3.121	0.053	0.113	−0.021	−0.022
	0.3	9.512	−0.064	0.537	−0.197	−0.212
2	0.05	0.605	0.001	0.001	0.001	0.001
	0.175	7.925	−0.008	−0.008	−0.008	−0.008
	0.3	27.551	−0.000	−0.000	−0.000	−0.000
3	0.05	−0.317	−0.002	−0.002	−0.002	−0.002
	0.175	−3.723	0.002	−0.010	0.002	0.002
	0.3	−10.224	−0.018	−0.072	−0.018	−0.018
4	0.05	0.044	−0.000	−0.002	−0.000	−0.000
	0.175	0.55	−0.001	−0.052	−0.001	−0.001
	0.3	1.641	0.005	−0.257	0.005	0.005

Table 3 Variance estimation for Gaussian bivariate input distribution expressed as percentage error with respect to the solution of a MCS with 5×10^7 samples

Case	$\sigma_{\mathbf{x}}$	I MM	II MM	III MM	S2	S3	URQ
1	0.05	0.341	0.592	0.090	−3.372	0.089	0.138
	0.175	3.147	6.306	−0.012	−11.434	0.972	1.589
	0.3	9.353	19.195	−0.489	−19.073	2.859	4.756
2	0.05	−1.282	−0.022	−0.022	1.142	−1.248	−0.022
	0.175	−13.498	0.022	0.022	−5.933	−13.132	0.022
	0.3	−31.488	−0.020	−0.020	−21.04	−30.638	−0.020
3	0.05	−0.204	−0.049	0.008	−2.029	−0.202	−0.064
	0.175	−2.540	−0.685	0.004	−8.468	−2.509	−0.868
	0.3	−7.177	−1.984	−0.056	−16.37	−7.088	−2.495
4	0.05	−0.113	0.026	−0.043	−4.917	−0.165	−0.186
	0.175	−0.847	0.846	0.003	−17.274	−1.483	−1.729
	0.3	−2.507	2.384	−0.050	−29.694	−4.327	−5.018

Table 5 Variance estimation for uniform bivariate input distribution expressed as percentage error with respect to the solution of a MCS with 5×10^7 samples

Case	$\sigma_{\mathbf{x}}$	I MM	II MM	III MM	S2	S3	URQ
1	0.05	0.282	0.458	0.057	−3.429	0.030	0.100
	0.175	2.930	5.137	0.093	−11.62	0.760	1.628
	0.3	8.609	15.451	−0.188	−19.623	2.160	4.797
2	0.05	−0.504	0.003	0.003	1.939	−0.470	0.003
	0.175	−5.862	0.023	0.023	2.370	−5.465	0.023
	0.3	−15.548	−0.033	−0.033	−2.669	−14.500	−0.033
3	0.05	−0.129	−0.058	−0.000	−1.955	−0.126	−0.073
	0.175	−1.550	−0.690	0.006	−7.538	−1.518	−0.874
	0.3	−4.482	−2.029	−0.045	−13.942	−4.390	−2.554
4	0.05	−0.101	0.017	−0.009	−4.906	−0.154	−0.152
	0.175	−1.113	0.323	0.005	−17.496	−1.747	−1.727
	0.3	−3.196	0.935	0.022	−30.191	−5.003	−4.948

Table 6 Mean estimation for generalized gamma (skewed) bivariate input distribution expressed as percentage error with respect to the solution of a MCS with 5×10^7 samples

Case	$\sigma_{\mathbf{x}}$	I MM	II MM	III MM	S2	URQ
1	0.05	0.253	0.009	0.007	−0.001	0.000
	0.175	3.198	0.127	0.037	−0.064	−0.024
	0.3	9.861	0.254	−0.227	−0.471	−0.246
2	0.05	0.604	0.000	0.000	0.000	0.000
	0.175	7.933	0.000	0.000	0.000	0.000
	0.3	27.551	0.000	0.000	0.000	0.000
3	0.05	−0.316	−0.001	−0.001	−0.001	−0.001
	0.175	−3.728	−0.003	−0.003	0.010	−0.003
	0.3	−10.221	−0.015	−0.015	0.052	−0.015
4	0.05	0.045	−0.000	−0.000	0.001	−0.000
	0.175	0.561	0.011	−0.001	0.062	−0.001
	0.3	1.697	0.061	0.000	0.323	0.000

observed, however, for quadratic functions with significant interactions (see Sec. III.B). In the asymmetric case, URQ has a better accuracy than I MM and S2, achieved by incorporating the term V_2 in Eq. (7). This is highlighted by the results of Table 7, particularly by those referring to the case of function 3. The results for functions 1 and 4 show the same behavior for $\boldsymbol{\sigma_{\mathbf{x}} = 0.05}$. When the input standard deviation increases, the effect of the interactions between variables becomes significant, and this reduces the accuracy of URQ for such cases.

V. Gradient-Based Robust Optimization

The proposed uncertainty propagation method gives deterministic estimates of $\mu_f, \sigma_f, \mu_{g_i}$, and σ_{g_i}, which are then suitably combined to form the robust objectives and constraints. Despite its underlying probabilistic formulation, the uncertainty propagation can be treated in a deterministic fashion, and the robust optimization can be dealt with by means of classical optimization algorithms. When the functions representing the deterministic response and/or constraints of the system are differentiable, the proposed propagation technique can be efficiently used in gradient-based optimization: since the robust objectives and constraints are not built using derivatives, their gradients are obtained through a combination of the deterministic gradients calculated at the sampling points defined by Eq. (22). Therefore, the equations of mean and variance sensitivities are, respectively,

$$\frac{\partial \mu_f}{\partial \mu_{x_q}} = W_0 \left.\frac{\partial f}{\partial x_q}\right|_{\boldsymbol{\mu}_{\mathbf{x}}} + \sum_{p=1}^{n} W_p \left(\frac{1}{h_p^+} \left.\frac{\partial f}{\partial x_q}\right|_{\mathbf{x}_p^+} - \frac{1}{h_p^-} \left.\frac{\partial f}{\partial x_q}\right|_{\mathbf{x}_p^-} \right) \tag{28}$$

$$\frac{\partial \sigma_f^2}{\partial \mu_{x_q}} = \sum_{p=1}^{n} \left(A_p \left.\frac{\partial f}{\partial x_q}\right|_{\mathbf{x}_p^+} + B_p \left.\frac{\partial f}{\partial x_q}\right|_{\mathbf{x}_p^-} - (A_p + B_p) \left.\frac{\partial f}{\partial x_q}\right|_{\boldsymbol{\mu}_{\mathbf{x}}} \right) \tag{29}$$

where

$$A_p = \frac{2W_p^+}{(h_p^+)^2}[f(\mathbf{x}_p^+) - f(\boldsymbol{\mu}_{\mathbf{x}})] + \frac{W_p^{\pm}}{h_p^+ h_p^-}[f(\mathbf{x}_p^-) - f(\boldsymbol{\mu}_{\mathbf{x}})]$$

$$B_p = \frac{2W_p^-}{(h_p^-)^2}[f(\mathbf{x}_p^-) - f(\boldsymbol{\mu}_{\mathbf{x}})] + \frac{W_p^{\pm}}{h_p^+ h_p^-}[f(\mathbf{x}_p^+) - f(\boldsymbol{\mu}_{\mathbf{x}})]$$

Requiring a single level of differentiation directly benefits gradient-based methods, the performance of which heavily depends on the accuracy of the supplied derivatives. This is because analytical expressions of objective functions and constraints are typically not available. These functions are often defined numerically, by means of computer programs. When the source code of such programs is available, one could use certain techniques to obtain exact derivatives, but this is usually only a viable option for the first derivatives. When the source code is not available, however, all derivatives required by the optimizer, and possibly those needed for building the robust functionals when using the MM, have to be determined by finite differencing. In this case, the major drawback of using the MM for the calculation of the robust functionals is the introduction of additional levels of differentiation, because each additional level leads to accumulation of truncation and roundoff errors. Among the possible approaches to the calculation of derivatives in the framework of robust gradient-based optimization, we mention the following three options:

1) For finite differences (FDs), the accuracy of the derivatives suffers from both truncation and roundoff errors, and such errors clearly increase if a double layer of derivation is required [58]. This would be the case if the uncertainty propagation were based on the first-order moment propagation. The situation becomes even worse when using quasi-Newton methods, in which the Hessian updates based on gradient evaluations may be corrupted due to the aforementioned inaccuracies. For a given common approach to the calculation of gradient and Hessian of robust objectives and

Table 7 Variance estimation for generalized gamma (skewed) bivariate input distribution expressed as percentage error with respect to the solution of a MCS with 5×10^7 samples

Case	$\sigma_{\mathbf{x}}$	I MM	II MM	III MM	S2	URQ
1	0.05	2.956	0.664	0.117	6.198	0.103
	0.175	13.032	6.927	−0.429	23.585	1.510
	0.3	26.949	20.404	−3.875	42.809	4.202
2	0.05	0.391	0.008	0.008	−2.039	0.008
	0.175	−10.649	0.003	0.003	−18.086	0.003
	0.3	−30.164	−0.020	−0.020	−39.947	−0.020
3	0.05	−2.821	−0.081	−0.025	−0.971	−0.096
	0.175	−10.912	−0.705	−0.075	−4.668	−0.871
	0.3	−19.872	−1.950	−0.285	−9.749	−2.390
4	0.05	0.824	0.113	0.029	5.729	−0.114
	0.175	2.145	0.926	−0.110	19.753	−1.823
	0.3	2.355	2.501	−0.551	32.924	−5.398

constraints, the URQ would result in smaller truncation and roundoff due to the lack of finite differencing in the analysis step.

2) For AD, currently, the computationally most convenient adjoint differentiation is well established for only gradient evaluation. If the linearization method were used, the evaluation of the Hessian would require the use of the computationally less effective forward AD mode. The AD technologies can be adopted only if source codes are available. Given that forward and backward AD are well established for only the calculation of lower-order derivatives, one notes again that derivative-free uncertainty propagation methods like URQ are likely to lead to smaller truncation and roundoff errors than derivative-based methods, because the latter ones are more likely to require finite differencing for evaluating robust functions of the gradients required by the optimizer.

3) For the CVM, this method is also applicable only if the source code is available, and it yields gradients with no roundoff errors; formulas for derivatives of order 2 and higher, however, involve the use of subtractions and, therefore, they are not immune from roundoff errors [59]. In view of this feature, the same remarks on truncation and roundoff errors made in the case of the AD approach are also applicable to the CVM case.

In all of the three aforementioned cases, there is no significant cost increase of the URQ-based robust optimization step with respect to the case in which I MM is used for the propagation phase. Considering a scalar function $y = f(\mathbf{x})$, in the most expensive case, when FDs are used to obtain the derivatives, such cost is $O(n^2)$, and it reduces to $O(n)$ in the best case, in which adjoint techniques are used for the first level of differentiation.

As mentioned previously, when the terms V_3 and V_4 in Eq. (7) are negligible (for example, when the input variables have weak cross interactions), the URQ variance estimate would exhibit an accuracy comparable with that of III MM at a computational cost comparable with that of I MM. In general, it would be useful to estimate, during the optimization, the error yielded by the terms V_3 and V_4 to keep under control the accuracy of the URQ propagation method. In the context of gradient-based optimization, and for the case in which the uncertain variables are a subset of the design variables, such accuracy monitoring can be achieved at no extra cost by using the derivatives calculated by the optimizer at each major optimization step. In fact, the higher-order derivatives appearing in the terms V_3 and V_4 can be approximated by FDs of the gradient values calculated on the URQ stencil, resulting in the following formulas:

$$V_3 \simeq \sum_{p=1}^{n} \sum_{\substack{q=1 \\ q \neq p}}^{n} \frac{(\partial x_q/\partial x_q)|_{\mathbf{x}_p^+} + (\partial f/\partial x_q)|_{\mathbf{x}_p^-} - 2(\partial f/\partial x_q)|_{\boldsymbol{\mu}_\mathbf{x}}}{(h_p^+ - h_p^-)^2} \frac{\partial f}{\partial x_q}\bigg|_{\boldsymbol{\mu}_\mathbf{x}} \sigma_{x_q}^2 \tag{30}$$

$$V_4 \simeq \frac{1}{8} \sum_{p=1}^{n} \sum_{\substack{q=1 \\ q \neq p}}^{n} \left[\frac{(\partial f/\partial x_q)|_{\mathbf{x}_p^+} - (\partial f/\partial x_q)|_{\mathbf{x}_p^-}}{(h_p^+ - h_p^-)\sigma_{x_p}} + \frac{(\partial f/\partial x_p)|_{\mathbf{x}_q^+} - (\partial f/\partial x_p)|_{\mathbf{x}_q^-}}{(h_q^+ - h_q^-)\sigma_{x_q}} \right]^2 \sigma_{x_p}^2 \sigma_{x_q}^2 \tag{31}$$

Being able to estimate the accuracy of the propagation phase constitutes a significant enhancement with respect to current practices based on the MM, for which the accuracy of the probabilistic estimates is checked, if at all, only at the optimal design point.

VI. Transonic Airfoil Design Optimization

In this section, the proposed URQ approach is applied to the problem of transonic airfoil design at the conceptual stage. The objective is to guarantee minimum sensitivity of the optimal aerodynamic performance with respect to variations of the geometry, which might occur at later stages of the development process (other sources of geometrical uncertainty can also be taken into account by RDO, as demonstrated in [60]). This test case concerns the optimization of an airfoil shape for transonic flight conditions. Three main components need to be combined for the study: 1) a geometry generation module, which creates the airfoil profile using a set of geometric design parameters; 2) a CFD code, which calculates the aerodynamic characteristics of the airfoil at hand; and 3) an optimization algorithm, which selects suitable values for the independent variables at each step of the optimization.

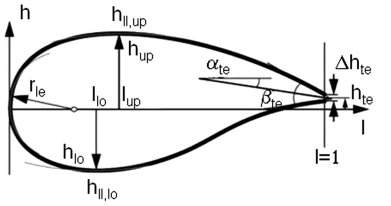

Fig. 1 PARSEC-11 geometry parameterization.

In the present study, these three modules have been wrapped by a MATLAB script that controls all phases of the design process and allows the MATLAB built-in gradient-based optimizer to be used for the problem at hand. The geometry parameterization and the CFD code are briefly described in the following subsections.

A. Geometry Generation

A variety of shape representation methods have been used in optimization studies. They include B splines [61,62], Hicks–Henne functions [63], Wagner functions [64], PARSEC-11 [65], and class shape transformation [66]. The choice of a particular technique is based on the technique's suitability for the application being considered. In the present work, we make use of the PARSEC-11 parameterization because of its intuitive airfoil description and the relatively small number of parameters it requires for defining the airfoil geometry. This method, developed by Sobieczky [65], is often used in airfoil and wing optimization. It makes use of a fractional-order polynomial to describe the (l, h) coordinates of the upper and lower surfaces of an airfoil:

$$h = \sum_{j=1}^{6} a_j(\mathbf{x}) l^{j-1/2} \tag{32}$$

where l varies between zero and one. The coefficients a_i of the polynomial are real and depend on the design vector $\mathbf{x}$ through simple mathematical relations. The design vector $\mathbf{x}$ is composed of 11 geometric parameters, such as radius of curvature, maximum crest value, and maximum crest location, as illustrated in Fig. 1. The parameters are described in Table 8, which also provides their bounds for the deterministic problem. In [67], Padulo et al. have highlighted some issues associated with the use of PARSEC-11 for airfoil geometry parametrization. In particular, we have shown that PARSEC-11 is sometimes prone to failures that may hinder both the uncertainty propagation and the optimization processes. To tackle such a problem, a methodology based on self-organizing maps and aiming to achieve a robust parameterization within the design space

Table 8 Considered design variables, airfoil test case

Design variable	Definition	Bounds $[\mathbf{x}_L, \mathbf{x}_U]$
r_{le}	Leading-edge radius	[0.005, 0.009]
l_{up}	Upper surface maximum crest location	[0.360, 0.450]
l_{lo}	Lower surface maximum crest location	[0.300, 0.560]
h_{up}	Upper surface maximum crest	[0.045, 0.057]
h_{lo}	Lower surface maximum crest	[−0.058, −0.040]
$h_{ll,up}$	Upper surface curvature at l_{up}	[−0.555, −0.260]
$h_{ll,lo}$	Lower surface curvature at l_{lo}	[0.280, 1.100]
h_{te}	Trailing-edge position	[−0.020, −0.009]
Δh_{te}	Trailing-edge thickness	[0.005, 0.008]
β_{te}	Trailing-edge aperture angle, deg	[0.100, 0.290]
α_{te}	Angle of trailing-edge bisector, deg	[−0.130, −0.080]

was proposed in [67]. The parametric space adopted for the study reported next was identified through the application of such methodology.

B. Computational Fluid Dynamics Code

The CFD code used for this study is viscous Garabedian–Korn (VGK) [68]. It can predict the aerodynamic characteristics of airfoils in subsonic freestream by coupling the full potential equations governing the inviscid flow region and the integral equations representing the viscous flow region. The code can also account for mild shocks by using an approximate form of the Rankine–Hugoniot equations. VGK has good accuracy for flows with attached boundary-layer weak shock waves with a Mach number before the shock smaller than 1.3, as assessed by means of comparisons of its results with those computed by other codes, and with experimental results [68,69]. This CFD code takes the user-provided lift as an input variable, and it determines, in an iterative fashion, the angle of attack for which such target lift is achieved. Other outputs of interest are the viscous and wave drag coefficients. The calculation of the former parameter is based on the far-field momentum thickness, applying the Cooke implementation of the Squire and Young approximation. The calculation of the latter parameter is accomplished by using Lock's second-order method.

The coupled potential and viscous equations are solved iteratively by means of a two-level grid-sequencing algorithm [68]. For the airfoil geometries considered in this study, the first four digits of the drag coefficient usually become constant after a total of 100 coarse-grid iterations and 300 fine-grid iterations. This is visible in Fig. 2a, which reports the convergence of the drag coefficient as a function of the fine-grid iteration count. This plot refers to the airfoil geometry used to initialize the optimization process. It should be noted that the convergence of the CVM-based first derivative of the drag with respect to the design variables is slightly slower than that of the drag itself. This is highlighted in Fig. 2b, which reports the derivative of the drag coefficient with respect to the leading-edge radius against the fine-grid iteration count. The first four digits of the derivatives of the drag coefficient usually become constant within 400 to 500 fine-grid iterations. To guarantee convergence of the drag coefficient and its derivatives, the number of iterations adopted for all the airfoil analyses required by the RDO, reported next, has been 200 for the coarse grid and 600 for the fine grid. Further details on the construction of the CVM derivatives in the VGK code are given in [53]. The developers of VGK originally conceived this program for interactive use only. The integration of VGK in the automated design optimization framework developed to perform the RDO exercise reported next has required the development of an interface to the MATLAB controller, including appropriate preprocessing and postprocessing modules. In particular, the postprocessing modules include suitable tests to verify the reliability of the VGK results and help the code converging for particularly difficult flow conditions resulting from the analysis of airfoils with fairly nonaerodynamic shapes. Such airfoil geometries may be encountered during intermediate stages of the optimization, but they are bypassed by the RDO framework, as they are found to not satisfy any optimality condition. The stability enhancement of VGK required to cope with the aforementioned unusual airfoils is achieved by automating the variation of numerical input parameter controlling stability and convergence of the calculation [70] (e.g., maximum number of iterations). No test is implemented to automatically verify the quality of the grid. The details of the implementation can be found in [71].

C. Formulation and Solution of the Robust Design Optimization Problem

The deterministic problem of interest is the minimization of the drag coefficient c_d with respect to the vector $\mathbf{x}$ specifying the PARSEC-11 parameters. The lift coefficient is fixed and, within the VGK analysis, the angle of attack to each considered airfoil is changed so that the same user-given lift coefficient is maintained. Two of the considered constraints regard the pitching moment coefficient c_m; the third and fourth prescribe a minimum thickness at 12 and 60% of the chord l, where the main spars are assumed to be located. The problem can be formulated as follows:

The objective is to minimize the drag coefficient c_d with respect to the design variables $\mathbf{x}$.

Constraints:

1) Pitching moment:

$$c_m > -0.10 \Rightarrow g_1 = -c_m - 0.10$$

2) Pitching moment:

$$c_m < -0.04 \Rightarrow g_2 = c_m + 0.04$$

3) Thickness at 12% l:

$$\text{thickness}_{12\%} > 0.076 \Rightarrow g_3 = -\text{thickness}_{12\%} + 0.076$$

4) Thickness at 60% l:

$$\text{thickness}_{60\%} > 0.072 \Rightarrow g_3 = -\text{thickness}_{60\%} + 0.072$$

The flight conditions considered are shown in Table 9.

The optimization of the airfoil shape is considered subject to uncertainty in the geometric parameters. The robust problem is hence set up by assigning a probability distribution to the 11 input variables, which is propagated to the probabilistic distributions of the objective function and the constraints. The input variables are described by independent Gaussian variables with a standard deviation equal to

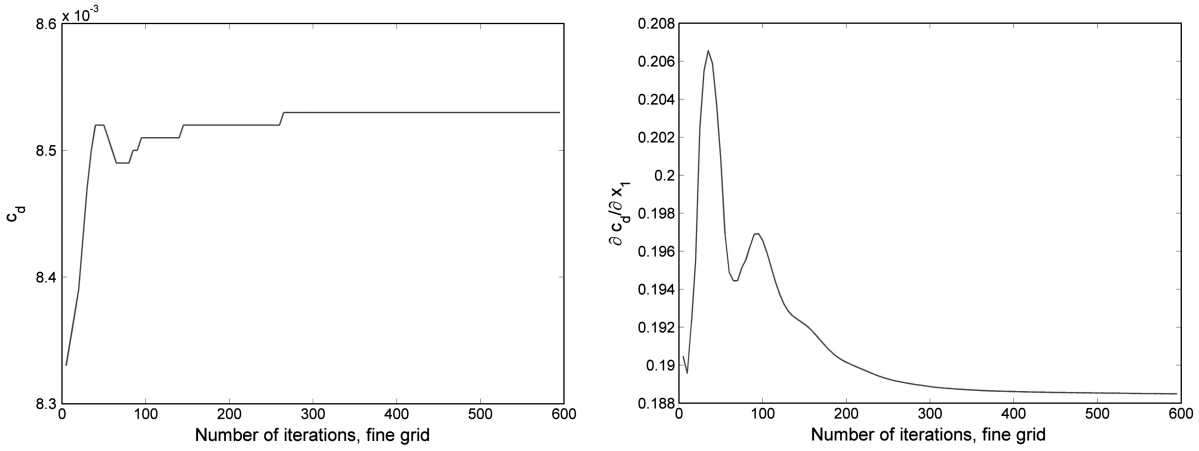

a) Calculated drag coefficient **b) CVM derivative $\partial c_d/\partial x_1$**

Fig. 2 Comparison of the convergence for the CFD output and its CVM derivative.

Table 9 Flight conditions and VGK settings

Parameter	Value
Mach number	0.72
Reynolds number	$21.1 \cdot 10^6$
Transition location, upper surface	1% chord
Transition location, lower surface	1% chord
Lift coefficient c_l	0.707

Table 10 Nominal features of RDO solutions and initial profile

Parameter	Initial profile	I MM	URQ
c_d	0.00852	0.00797	0.00784
c_l	0.70697	0.70702	0.70704
c_m	−0.06263	−0.09371	−0.09488
$\text{thickness}_{12\%}$	0.07769	0.07688	0.07683
$\text{thickness}_{60\%}$	0.07361	0.08909	0.09083
angle of attack α, deg	1.860	1.191	0.954

3% of the input variable ranges. Such a coefficient of variation for $\mathbf{x}$ corresponds to a coefficient of variation of 7% for both the maximum thickness and the camber, which can be considered appropriate for the conceptual phase of the airfoil definition. The initial profile is derived from previous studies considering different flight conditions. The mathematical problem to be solved is hence formulated as in Eq. (2), where the adopted coefficients are $k_f = \sqrt{2}$, $k_{\mathbf{x}} = 1$, and $k_{g_i} = 1.22$, for $i = 1, \ldots, 4$. To demonstrate the validity of the URQ-based propagation strategy in the context of gradient-based optimization, we proceed to compare its results against those obtained with the frequently used first-order MM for the design problem at hand. Such comparison is performed by carrying out two different optimizations: the first using I MM and the second the URQ technique.

The gradient-based optimizer that we have used is FMINCON, which is the constrained nonlinear optimizer of the MATLAB Optimization Toolbox [72]. This algorithm uses a sequential quadratic programming method, in which a quadratic programming subproblem is solved at each iteration. A quasi-Newton estimate of the Hessian of the Lagrangian is obtained by using the Broyden–Fletcher–Goldfarb–Shanno formula. The convergence of this algorithm is superlinear with respect to the optimization steps when dealing with smooth functions. Further details on the algorithmic features of FMINCON can be found in [72].

To unequivocally attribute the discrepancies between the two optimization processes and results to the adopted propagation methods only, we use a common procedure for calculating all the derivatives required by the optimizer in both URQ and I MM optimizations. The first derivatives required by FMINCON have been computed using the accurate CVM in both optimization setups, so as to ensure the same accuracy for the calculation of all the derivatives used to steer the two optimizations. The calculation of the URQ-based robust functions is derivative free; the calculation of the moment-based robust functions, conversely, requires derivatives, which have been determined by means of finite differences. As previously mentioned, this is a significant drawback of moment methods because, in most practical design problems, it may be hard to avoid the numerical noise due to the roundoff errors associated with finite differencing. An additional related problem is the choice of an optimal step for finite differencing. This parameter should not be too small, to avoid excessive roundoff errors, or too large, to prevent the truncation error from growing without bounds. Optimal ranges often do not exist due to strong nonlinearity of the function at hand. Preliminary studies were carried out in the attempt of determining optimal differencing steps to be used in the I MM-based optimization discussed in the following section. This aspect is thoroughly discussed and documented in [53].

D. Results

The I MM and the URQ optimization exercises result in two different optimal profiles. The characteristics of the initial airfoil, and those of the two new airfoils obtained by means of the URQ-based and I MM-based RDOs, are reported in Table 10. The solution given by the URQ optimization has lower drag than that found when the I MM is employed. This is due to the more effective reduction of the shock located on the upper surface of the initial airfoil at approximately $l = 0.35$ (Fig. 3b). As visible in Fig. 3a, the main geometrical differences between the two robust optima regard the trailing edge and the curvature of the rear upper and upper parts of the airfoil.

Figure 4a shows that, when the URQ quadrature is adopted for the uncertainty propagation, the optimizer converges to the solution in fewer iterations than in the case of uncertainty propagation based on I MM, and it does so without the strong oscillations of the expectation of the objective function observed in the I MM case. The smoother convergence of the URQ-based optimization is due to the fact that the numerical noise of objective functions and constraints is smoothed to a larger extent when using an integral approach (as URQ does) rather than a differential approach (as I MM does) to the propagation of uncertainty. The larger sampling step of the URQ approach, which depends on the input moments as indicated by Eq. (22), results in enhanced smoothing of the numerical noise. Conversely, such noise spoils the accuracy of any finite difference in the I MM case. Figure 4b shows how the error estimate of the variance of the objective function relative to the third-order MM, obtained by means of Eqs. (30) and (31), varies during the optimization. The final error estimate of the variance is about 2%, and we also observe that the

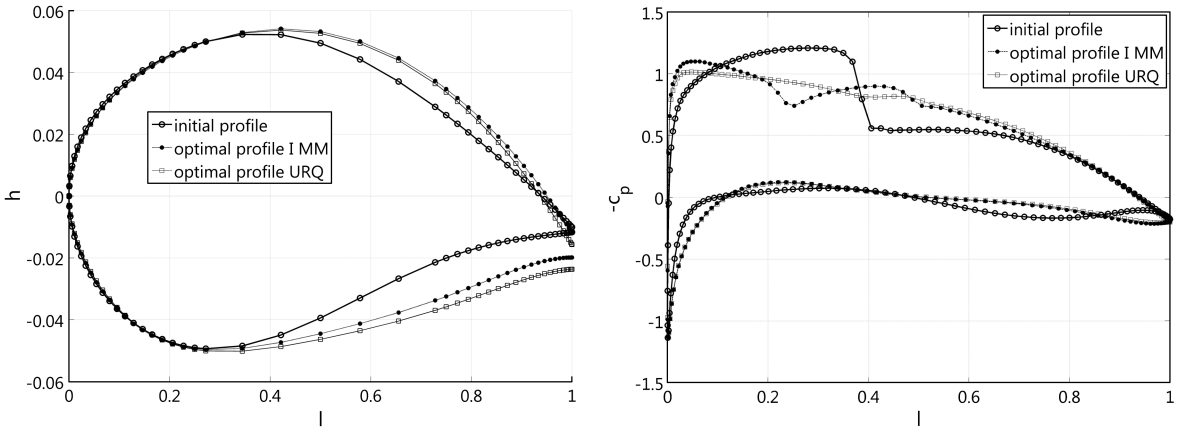

a) Airfoil geometry **b) Pressure distribution**

Fig. 3 Robust optimizations solutions compared with the initial profile.

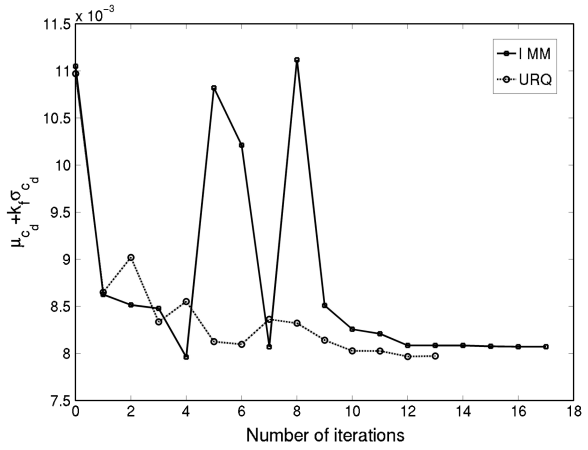

a) Convergence of the two optimizations

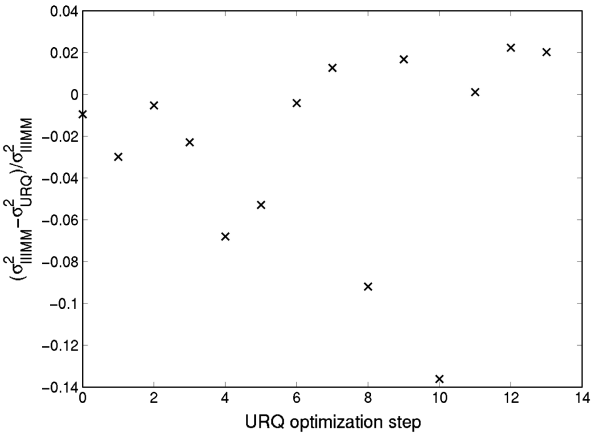

b) $\sigma^2_{f_{\mathrm{URQ}}}$ error during the optimization

Fig. 4 I MM and URQ optimizations.

error estimate occasionally exceeds 10% before the optimal solution is achieved. The magnitude of this error could be due to local strong nonlinearities of the deterministic objective function. In the course of other optimization exercises (not reported herein), we have sometimes observed that the errors indicated by this error estimator were higher than those visible in Fig. 4b. In these circumstances, a suitable higher-order quadrature method should be adopted to improve the accuracy of the variance of the objective functions and/or constraints.

To assess the robustness of the two optima and analyze their features in more detail, a postoptimal analysis is performed by means of a MCS (Latin hypercube with 6000 samples). The two optima $\mathbf{x}_{\mathrm{opt}}$ are represented again as Gaussian random variables with variances equal to that used throughout the two optimizations. Figure 5a shows that the URQ-based optimal design outperforms the I MM-based one in terms of drag robust optimality, as both the mean and the variance of the former are lower than those associated with the latter. The statistical distribution of the pitching moment associated with the initial geometry and the two robust optima is depicted in Fig. 5b, whereas the distribution of the thickness induced by the robust optimization at the location where the two constraints have been enforced can be observed in Figs. 5c and 5d.

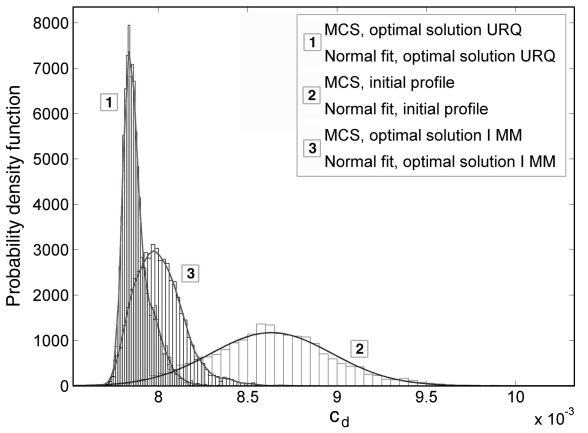

a) Objective: drag coefficient

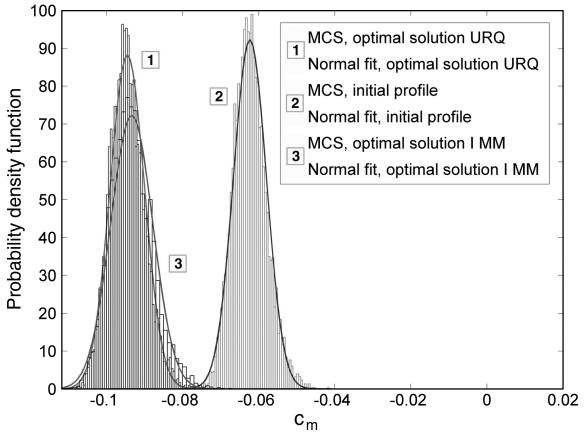

b) Constraint: pitching moment coefficient

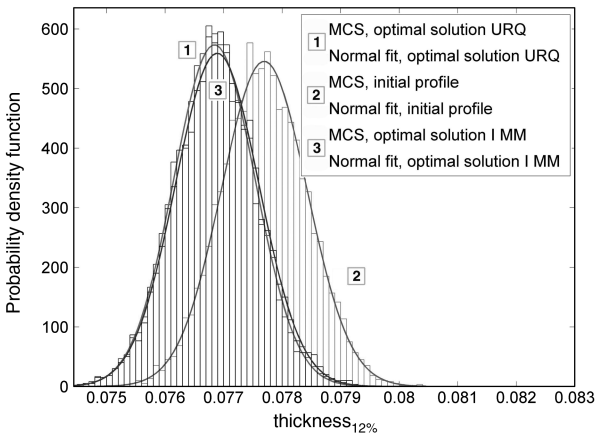

c) Constraint: thickness at 12% chord

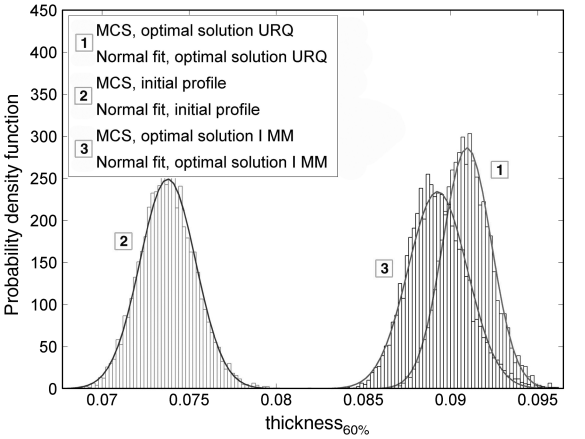

d) Constraint: thickness at 60% chord

Fig. 5 MCS validation of optimal results.

Table 11 Postoptimality analysis: relative error on mean and variance estimation of objective and constraints with respect to MCS

Objective/ constraint	Mean estimation		Variance estimation	
	$x_{\text{opt,IMM}}$	$x_{\text{opt,URQ}}$	$x_{\text{opt,IMM}}$	$x_{\text{opt,URQ}}$
c_d	0.43×10^{-2}	-0.15×10^{-3}	0.72	−0.14
c_m	-0.38×10^{-2}	-0.18×10^{-3}	0.20	0.18×10^{-1}
$\text{thickness}_{12\%}$	0.18×10^{-4}	0.24×10^{-5}	0.10×10^{-1}	-0.02×10^{-2}
$\text{thickness}_{60\%}$	-0.62×10^{-4}	0.69×10^{-5}	0.71×10^{-1}	-0.86×10^{-2}

The first and third columns of Table 11 report the percentage difference between the I MM-based optimum and its MCS reconstruction. The first column refers to the mean, and the third refers to the variance. The second and fourth columns report the percentage difference between the URQ-based optimum and its MCS reconstruction in terms of the same variables. These results highlight the significantly higher accuracy of the URQ approach with respect to the linearization method. It should also be noted that the computational cost associated with the evaluation of the robust objectives and constraints accomplished by the two methods is comparable, and in this particular problem, the URQ-based optimization requires fewer iterations than the I MM one. This is presumably due to the noise associated with the truncation error of the finite differences used to evaluate the moments of objectives and constraints.

VII. Conclusions

Presented in this paper is a novel uncertainty propagation technique based on a URQ rule. The method allows one to construct deterministic estimates of the mean and variance of nonlinear functions computed by analysis codes of any complexity. The use of such a technique requires a computational cost comparable to that of the linearization method, but it allows a higher accuracy to be achieved. Moreover, the derivative-free nature of the URQ is advantageous with respect to linearization in the context of gradient-based optimization, since a URQ robust optimization procedure requires one less level of differentiation with respect to the case of uncertainty propagation based on first derivatives.

Further benefits of the method include the ease of implementation, since the sampling step is entirely determined on the basis of the input distribution, and its ability to deal with CFD noise, which may ultimately complicate the optimization process. Furthermore, the URQ approach does not require the source code that performs the deterministic analysis and, for this reason, can also be easily used with commercial analysis software.

By solving a robust optimization problem focusing on the conceptual design of a transonic airfoil, it has been shown that the solutions obtained using the URQ approach to uncertainty propagation can outperform those obtained using the linearization method. It has also been shown how the error with respect to methods based on higher-order Taylor-series expansion can be kept under control during the optimization phase. In the study reported herein, this feature is used only to monitor accuracy as the optimization process progresses. Future work will investigate the possibility of using higher-order quadrature rules at points of the design space where the mean and variance errors exceeds predefined thresholds. The proposed URQ-based uncertainty propagation methodology is fairly general and can be applied to a broad range of design optimization problems of multidisciplinary nature.

Appendix: Accuracy of the Univariate Reduced Quadrature Propagation Method

The idea behind the development of the URQ method is to provide an integration formula for solving Eqs. (3) and (4) by matching the highest possible number of terms of the mean and variance expressions based on a third-order Taylor-series expansion. The complete representations of mean and variance based on such Taylor expansion are provided by Eqs. (6) and (7), respectively. In analogy with Gauss-type quadrature formulas [73], our formulas can be written as weighted sums of functional values. By considering two nodes for each dimension of the input space D, with $D \subseteq \mathbb{R}^n$, plus a central point corresponding to the mean $\boldsymbol{\mu}_{\mathbf{x}}$, one can write the following expressions:

$$\mu_f = W_0 f(\boldsymbol{\mu}_{\mathbf{x}}) + \sum_{p=1}^{n} [W_A f(\mathbf{x}_p^+) + W_B f(\mathbf{x}_p^-)] \tag{A1}$$

$$\sigma_f^2 = \sum_{p=1}^{n} \{W_a [f(\mathbf{x}_p^+) - f(\boldsymbol{\mu}_{\mathbf{x}})]^2 + W_b [f(\mathbf{x}_p^-) - f(\boldsymbol{\mu}_{\mathbf{x}})]^2 + W_c [f(\mathbf{x}_p^+) - f(\boldsymbol{\mu}_{\mathbf{x}})][f(\mathbf{x}_p^-) - f(\boldsymbol{\mu}_{\mathbf{x}})]\} \tag{A2}$$

The sampling points are defined as follows:

$$\mathbf{x}_p^{\pm} = \boldsymbol{\mu}_{\mathbf{x}} + h_p^{\pm} \sigma_{x_p} \mathbf{e}_p \tag{A3}$$

To simplify the notation, in the following, it is assumed (without any loss of generality) that $\boldsymbol{\sigma}_{\mathbf{x}} = \mathbf{1}$. Suppose that f is analytic on the range $[\mathbf{x}_p^-, \mathbf{x}_p^+]$. Therefore, the functional values $f(\mathbf{x}_p^+)$ and $f(\mathbf{x}_p^-)$ can be written by means of a Taylor-series expansion centered at $\boldsymbol{\mu}_{\mathbf{x}}$, leading to the following equations:

$$f(\mathbf{x}_p^+) = f(\boldsymbol{\mu}_{\mathbf{x}}) + \sum_{i=1}^{\infty} \frac{\partial^i f}{\partial x_p^i} \frac{(h_p^+)^i}{i!} \tag{A4}$$

$$f(\mathbf{x}_p^-) = f(\boldsymbol{\mu}_{\mathbf{x}}) + \sum_{i=1}^{\infty} \frac{\partial^i f}{\partial x_p^i} \frac{(h_p^-)^i}{i!} \tag{A5}$$

Substituting Eqs. (A4) and (A5) into Eqs. (A1) and (A2), the following equations are obtained:

$$\mu_f = W_0 f(\boldsymbol{\mu}_{\mathbf{x}}) + \sum_{p=1}^{n} \left[f(\boldsymbol{\mu}_{\mathbf{x}})(W_A + W_B) + \sum_{i=1}^{\infty} \frac{\partial^i f}{\partial x_p^i} \frac{W_A (h_p^+)^i + W_B (h_p^-)^i}{i!} \right] \tag{A6}$$

$$\sigma_f^2 = \sum_{p=1}^{n} \sum_{i=1}^{\infty} \sum_{j=1}^{\infty} \frac{\partial^i f}{\partial x_p^i} \frac{\partial^j f}{\partial x_p^j} \frac{W_a (h_p^+)^{i+j} + W_b (h_p^-)^{i+j} + W_c (h_p^+)^i (h_p^-)^j}{i! j!} \tag{A7}$$

These equations are the URQ approximations of mean and variance. Their accuracy depends on the value chosen for the weights W_0, W_A, W_B, W_a, W_b, and W_c, and for the sampling locations identified by h_p^+ and h_p^-. To find the best values for such parameters, one needs eight conditions. These can be obtained by equating Eqs. (A6) and (A7) to Eqs. (6) and (7), respectively. One can observe that it is possible to resolve the terms $M1$, $M2$, $M3$, and $M4$ in Eq. (6) and the terms $V1$, $V2$, $V5$, and $V6$ in Eq. (7). The terms $M5$, $V3$, and $V4$ cannot be resolved, since Eqs. (A6) and (A7) do not feature cross-derivative terms. These conditions lead to the following system of equations:

$$\begin{cases} W_0 + \sum_{p=1}^{n}(W_A + W_B) = 1 \\ W_A h_p^+ + W_B h_p^- = 0 \\ W_A (h_p^+)^2 + W_B (h_p^-)^2 = 1 \\ W_A (h_p^+)^3 + W_B (h_p^-)^3 = \gamma_{x_p} \\ W_A (h_p^+)^4 + W_B (h_p^-)^4 = \Gamma_{x_p} \\ W_a (h_p^+)^2 + W_b (h_p^-)^2 + W_c h_p^+ h_p^- = 1 \\ W_a (h_p^+)^3 + W_b (h_p^-)^3 + \frac{W_c}{2}[(h_p^+)^2 h_p^- + h_p^+ (h_p^-)^2] = \gamma_{x_p} \\ W_a (h_p^+)^4 + W_b (h_p^-)^4 + \frac{W_c}{2}[(h_p^+)^3 h_p^- + h_p^+ (h_p^-)^3] = \Gamma_{x_p} \\ W_a (h_p^+)^4 + W_b (h_p^-)^4 + W_c (h_p^+)^2 (h_p^-)^2 = \Gamma_{x_p} - 1 \end{cases} \tag{A8}$$

It can be shown that the sixth, seventh, and eighth equations of this system are linearly dependent, and that only two equations among these are independent. Discarding one of these three equations, we are left with eight independent equations that uniquely determine the eight parameters identifying the weights and the sampling locations. The solution of the system is

$$h_p^{\pm} = \frac{\gamma_{x_p}}{2} \pm \sqrt{\Gamma_{x_p} - \frac{3\gamma_{x_p}^2}{4}} \tag{A9}$$

and

$$W_0 = 1 + \sum_{p=1}^{n} \frac{1}{h_p^+ h_p^-}; \qquad W_A = \frac{1}{h_p^+ (h_p^+ - h_p^-)}$$

$$W_B = -\frac{1}{h_p^- (h_p^+ - h_p^-)}; \qquad W_a = \frac{(h_p^+)^2 - h_p^+ h_p^- - 1}{(h_p^+)^2 (h_p^+ - h_p^-)^2}$$

$$W_b = \frac{(h_p^-)^2 - h_p^+ h_p^- - 1}{(h_p^-)^2 (h_p^+ - h_p^-)^2}; \qquad W_c = \frac{2}{h_p^+ h_p^- (h_p^+ - h_p^-)^2}$$

After some simple algebraic manipulation on the expressions of the weights, we can rewrite Eqs. (A1) and (A7) and the expressions of the weights as in Sec. III.

Acknowledgment

The research reported in this paper has been partly sponsored by the European Union Integrated Project: Value Improvement Through a Virtual Aeronautical Collaborative Enterprise (AIP3 CT-2003-502917).

References

[1] Chen, W., and Allen, J., "A Procedure for Robust Design: Minimizing Variations Caused by Noise Factors and Control Factors," *Journal of Mechanical Design*, Vol. 118, No. 4, 1996, pp. 478–493. doi:10.1115/1.2826915

[2] Phadke, M. S., *Quality Engineering Using Robust Design*, Prentice–Hall, Englewood Cliffs, NJ, 1989.

[3] Park, G. J., Lee, T. H., Lee, K. H., and Hwang, K. H., "Robust Design: An Overview," *AIAA Journal*, Vol. 44, No. 1, 2006, pp. 181–191. doi:10.2514/1.13639

[4] Stroud, A. H., "Remarks on the Disposition of Points in Numerical Integration Formulas," *Mathematics of Computation*, Vol. 11, No. 60, 1957, pp. 257–261. doi:10.1090/S0025-5718-1957-0093911-3

[5] Stroud, A. H., "Numerical Integration Formulas of Degree Two," *Mathematics of Computation*, Vol. 14, No. 69, 1960, pp. 21–26. doi:10.1090/S0025-5718-1960-0109977-8

[6] Xiu, D., "Numerical Integration Formulas of Degree Two," *Applied Numerical Mathematics*, Vol. 58, No. 10, 2008, pp. 1515–1520. doi:10.1016/j.apnum.2007.09.004

[7] Parkinson, A., Sorensen, C., and Pourhassan, "A General Approach for Robust Optimal Design," *Journal of Mechanical Design*, Vol. 115, No. 1, 1993, pp. 74–80. doi:10.1115/1.2919328

[8] Lewis, L., and Parkinson, A., "Robust Optimal Design Using a Second Order Tolerance Model," *Research in Engineering Design*, Vol. 6, No. 1, 1994, pp. 25–37. doi:10.1007/BF01588089

[9] Du, X., and Chen, W., "Efficient Uncertainty Analysis Methods for Multidisciplinary Robust Design," *AIAA Journal*, Vol. 40, No. 3, 2002, pp. 545–552. doi:10.2514/2.1681

[10] Putko, M., Newman, P., Taylor, A., and Green, L., "Approach for Uncertainty Propagation and Robust Design in CFD Using Sensitivity Derivatives," Proceedings of the 15th AIAA Computational Fluid Dynamics Conference, Anaheim CA, AIAA Paper 2001-2528, June 2001.

[11] Green, L. L., Lin, H., and Khalessi, M. R., "Probabilistic Methods for Uncertainty Propagation Applied to Aircraft Design," 20th AIAA Applied Aerodynamics Conference, St. Louis, MO, AIAA Paper 2002-3140, June 2002.

[12] Martinelli, M., and Duvigneau, R., "Comparison of Second-Order Derivatives and Metamodelbased Monte-Carlo Approaches to Estimate Statistics for Robust Design of a Transonic Wing," 49th AIAA/ASCE/AHS/ASC Structures, Structural Dynamics, and Materials Conference, Schaumburg, IL, AIAA Paper 2008-2071, April 2008.

[13] Barthelemy, J. F., and Hall, L. E., "Automatic Differentiation as a Tool in Engineering Design," NASA, TM 107661, Aug. 1992.

[14] Griewank, A., "A Mathematical View of Automatic Differentiation," *Acta Numerica*, Vol. 12, 2003, pp. 321–398. doi:10.1017/S0962492902000132

[15] Griewank, A., "On Automatic Differentiation," *Mathematical Programming: Recent Developments and Applications*, edited by M. Iri and K. Tanabe, Kluwer Academic, Dordrecht, The Netherlands, 1989, pp. 83–108.

[16] Su, J., and Renaud, J. E., "Automatic Differentiation in Robust Optimization," *AIAA Journal*, Vol. 35, No. 6, 1997, pp. 1072–1079. doi:10.2514/2.196

[17] Martins, J. R. R. A., Sturdza, P., and Alonso, J. J., "The Complex-Step Derivative Approximation," *ACM Transactions on Mathematical Software*, Vol. 29, No. 3, 2003, pp. 245–262. doi:10.1145/838250.838251

[18] Taguchi, G., "Performance Analysis Design," *International Journal of Production Research*, Vol. 16, No. 6, 1978, pp. 521–530. doi:10.1080/00207547808930043

[19] D'Errico, J. R., and Zaino, N. A., Jr., "Statistical Tolerancing Using a Modification of Taguchi's Method," *Technometrics*, Vol. 30, No. 4, 1988, pp. 397–405. doi:10.2307/1269802

[20] Seo, H. S., and Kwak, B. M., "Efficient Statistical Tolerance Analysis for General Distributions Using Three-Point Information," *International Journal of Production Research*, Vol. 40, No. 4, 2002, pp. 931–944. doi:10.1080/00207540110095709

[21] Huang, B., and Du, X., "A Robust Design Method Using Variable Transformation and Gauss–Hermite Integration," *International Journal for Numerical Methods in Engineering*, Vol. 66, No. 12, 2006, pp. 1841–1858. doi:10.1002/nme.1577

[22] Evans, D. H., "Statistical Tolerancing: The State of the Art, Part II," *Journal of Quality Technology*, Vol. 7, No. 1, 1975, pp. 1–12.

[23] Julier, S. J., and Uhlmann, J. K., "A General Method for Approximating Nonlinear Transformations of Probability Distributions," Univ. of Oxford, Robotic Research Group, Dept. of Engineering Science, TR., U.K., Nov. 1996.

[24] Nørgaard, M., Poulsen, N. K., and Ravn, O., "Advances in Derivative-Free State Estimation for Nonlinear Systems," Technical Univ. of Denmark, Department of Mathematical Modelling, TR IMM-REP 1998-15, Denmark, April 2000.

[25] Padulo, M., Campobasso, M. S., and Guenov, M. D., "Comparative Analysis of Uncertainty Propagation Methods for Robust Engineering Design," *International Conference on Engineering Design ICED07* [CD-ROM], Paris, Professional Engineering Publ., London, U.K., Aug. 2007.

[26] Cioffi, M., Formisano, A., Martone, R., Steiner, G., and Watzenig, G., "A Fast Method for Statistical Robust Optimization," *IEEE Transactions on Magnetics*, Vol. 42, No. 4, 2006, pp. 1099–1102. doi:10.1109/TMAG.2006.871983

[27] Xu, H., and Rahman, S., "A Generalized Dimension-Reduction Method for Multidimensional Integration in Stochastic Mechanics," *International Journal for Numerical Methods in Engineering*, Vol. 61, No. 12, 2004, pp. 1992–2019. doi:10.1002/nme.1135

[28] Rahman, S., and Xu, H., "A Univariate Dimension-Reduction Method for Multidimensional Integration in Stochastic Mechanics," *Probabilistic Engineering Mechanics*, Vol. 19, No. 4, 2004, pp. 393–408. doi:10.1016/j.probengmech.2004.04.003

[29] Huang, B., and Du, X., "Uncertainty Analysis by Dimension Reduction Integration and Saddlepoint Approximations," *Transactions of the ASME*, Vol. 128, No. 1, 2006, pp. 26–33. doi:10.1115/1.2118667

[30] Youn, B. D., Xi, Z., Wells, L. J., and Wang, P., "Enhanced Dimension-Reduction (eDR) Method for Sensitivity-Free Uncertainty Quantification," 11 th AIAA/ISMO Multidisciplinary Analysis and Optimization Conference, Portsmouth, VA, AIAA Paper 2006-6977, Sept. 2006.

[31] Lee, S. H., and Chen, W., "A Comparative Study of Uncertainty Propagation Methods for Black-Box-Type Problems," *Structural and Multidisciplinary Optimization*, Vol. 37, No. 3, 2008, pp. 239–253. doi:10.1007/s00158-008-0234-7

[32] Lee, S., Chen, W., and Kwak, B., "Robust Design with Arbitrary Distributions Using Gauss-Type Quadrature Formula," *Structural and Multidisciplinary Optimization*, Vol. 39, No. 3, 2008, pp. 227–243. doi:10.1007/s00158-008-0328-2

[33] Lee, I., Choi, K. K., Du, L., and Gorsich, D., "Dimension Reduction Method for Reliability-Based Robust Design Optimization," *Computers and Structures*, Vol. 86, Nos. 13–14, 2008, pp. 1550–1562. doi:10.1016/j.compstruc.2007.05.020

[34] Hammersley, J. M., and Handscomb, D. C., *Monte Carlo Methods*, Chapman and Hall, New York, 1964.

[35] Helton, J. C., and Davis, F. J., "Latin Hypercube Sampling and the Propagation of Uncertainty In Analyses of Complex Systems," *Reliability Engineering and System Safety*, Vol. 81, No. 1, 2003, pp. 23–69. doi:10.1016/S0951-8320(03)00058-9

[36] Tari, M., and Dahmani, A., "Refined Descriptive Sampling: A better Approach to Monte Carlo Simulation," *Simulation Modelling Practice and Theory*, Vol. 14, No. 2, 2006, pp. 143–160. doi:10.1016/j.simpat.2005.04.001

[37] Caisch, R. E., "Monte Carlo and Quasi-Monte Carlo Methods," *Acta Numerica*, Vol. 7, 1998, pp. 1–49. doi:10.1017/S0962492900002804

[38] Beyer, H., and Sendhoff, B., "Robust Optimization: A Comprehensive Survey," *Computer Methods in Applied Mechanics and Engineering*, Vol. 196, Nos. 33–34, 2007, pp. 3190–3218. doi:10.1016/j.cma.2007.03.003

[39] Rayward-Smith, V. J., Osman, I. H., Reeves, C. R., and Smith, G. D. (eds.), *Modern Heuristic Search Methods*, Wiley, Chichester, U.K., 1996, pp. 255–272.

[40] Back, T., Hammel, U., and Schwefel, H. P., "Evolutionary Computation: Comments on the History and Current State," *IEEE Transactions on Evolutionary Computation*, Vol. 1, No. 1, April 1997, pp. 3–17. doi:10.1109/4235.585888

[41] Robbins, H., and Monro, S., "A Stochastic Approximation Method," *Annals of Mathematical Statistics*, Vol. 22, No. 3, 1951, pp. 400–407. doi:10.1214/aoms/1177729586

[42] Ermoliev, Y., "Stochastic Quasi-Gradients Methods," *Numerical Techniques for Stochastic Optimization*, edited by Y. Ermoliev, Springer–Verlag, Berlin, 1988, pp. 141–185, Chap. 6.

[43] Sadegh, P., and Spall, J. C., "Optimal Random Perturbations for Stochastic Approximation Using a Simultaneous Perturbation Gradient Approximation," *IEEE Transactions on Automatic Control*, Vol. 43, No. 10, Oct. 1998, pp. 1480–1484. doi:10.1109/9.720513

[44] Kolda, T. G., Lewis, R. M., and Torczon, V., "Optimization by Direct Search: New Perspectives on Some Classical and Modern Methods," *SIAM Review*, Vol. 45, No. 3, 2003, pp. 385–482. doi:10.1137/S003614450242889

[45] Fletcher, R., *Practical Methods of Optimization*, 2nd ed., Wiley, New York, 1987.

[46] Ghanem, R. G., and Spanos, P. D., *Stochastic Finite Elements: A Spectral Approach*, Dover, London, 1991.

[47] Mathelin, L., Hussaini, M. Y., and Zang, T. A., "Stochastic Approaches to Uncertainty Quantification in CFD Simulations," *Numerical Algorithms*, Vol. 38, Nos. 1–3, 2005, pp. 209–236. doi:10.1007/BF02810624

[48] Rosenblatt, M., "Remarks on a Multivariate Transformation," *Annals of Mathematical Statistics*, Vol. 23, No. 3, 1952, pp. 470–472. doi:10.1214/aoms/1177729394

[49] Xiu, D., and Karniadakis, E. M., "Modeling Uncertainty in Flow Simulations via Generalized Polynomial Chaos," *Journal of Computational Physics*, Vol. 187, No. 1, 2003, pp. 137–167. doi:10.1016/S0021-9991(03)00092-5

[50] Eldred, M. S., and Burkardt, J., "Comparison of Non-Intrusive Polynomial Chaos and Stochastic Collocation Methods for Uncertainty Quantification," 47th AIAA Aerospace Sciences Meeting including the New Horizons Forum and Aerospace Exposition, Orlando, FL, AIAA Paper 2009-0976, Jan. 2009.

[51] Eldred, M. S., Webster, C. G., and Constantine, P. G., "Design Under Uncertainty Employing Stochastic Expansion Methods," 12th AIAA/ISSMO Multidisciplinary Analysis and Optimization Conference. 2008, Victoria, B.C., Canada, AIAA Paper 2008-6001, Sept. 2008.

[52] Lurati, L. B., "Robust Airfoil Design Under Uncertain Operation Conditions Using Stochastic Collocation," 46th AIAA Aerospace Sciences Meeting and Exhibit, Reno, NV, AIAA Paper 2008-0135, Jan. 2008.

[53] Padulo, M., "Computational Engineering Design Under Uncertainty: An Aircraft Conceptual Design Perspective," Ph.D. Thesis, Cranfield Univ., Cranfield, England, U.K., 2009.

[54] Jaeckel, P., "A Note on Multivariate Gauss–Hermite Quadrature," May 2005, http://www. otc-analytics.com-a.googlepages .com/ANoteOnMultivariateGaussHermiteQuadr.pdf [retrieved 30 June 2009].

[55] Nelsen, R. B., *An Introduction to Copulas*, Springer, New York, 2006.

[56] Clemen, R. T., and Reilly, T., "Correlations and Copulas for Decision and Risk Analysis," *Management Science*, Vol. 45, No. 2, 1999, pp. 208–224. doi:10.1287/mnsc.45.2.208

[57] Nørgaard, M., Poulsen, N. K., and Ravn, O., "New Developments in State Estimation of Nonlinear Systems," *Automatica*, Vol. 36, No. 11, Nov. 2000, pp. 1627–1638. doi:10.1016/S0005-1098(00)00089-3

[58] Padulo, M., Forth, S. A., and Guenov, M. D., "Robust Aircraft Conceptual Design Using Automatic Differentiation in Matlab," *Advances in Automatic Differentiation*, edited by C. H. Bischof, H. M. Bücker, P. D. Hovland, U. Naumann, and J. Utke, Springer, New York, 2008, pp. 271–280.

[59] Lai, K. L., and Crassidis, J. L., "Extensions of the First and Second Complex-Step Derivative Approximations," *Journal of Computational and Applied Mathematics*, Vol. 219, No. 1, 2008, pp. 276–293. doi:10.1016/j.cam.2007.07.026

[60] Keane, A. J., "Comparison of Several Optimization Strategies for Robust Turbine Blade Design," *Journal of Propulsion and Power*, Vol. 25, No. 5, 2009, pp. 1092–1099. doi:10.2514/1.38673

[61] Cosentino, G. B., and Holst, T. L., "Numerical Optimization Design of Advanced Transonic Wing Configurations," *Journal of Aircraft*, Vol. 23, No. 3, 1986, pp. 192–199. doi:10.2514/3.45288

[62] Lepine, J., Guibault, F., Trepanier, J. Y., and Pepin, F., "Optimized Nonuniform Rational B-Spline Geometrical Representation for Aerodynamic Design of Wings," *AIAA Journal*, Vol. 39, No. 11, 2001, pp. 2033–2041. doi:10.2514/2.1206

[63] Hicks, R. M., and Henne, P. A., "Wing Design by Numerical Optimisation," *Journal of Aircraft*, Vol. 15, No. 7, 1978, pp. 407–412. doi:10.2514/3.58379

[64] Ramamoorthy, P., and Padmavathi, K., "Airfoil Design by Optimization," *Journal of Aircraft*, Vol. 14, No. 2, 1977, pp. 219–221. doi:10.2514/3.44587

[65] Sobieczky, H., "Parametric Airfoils and Wings," *Notes on Numerical Fluid Mechanics*, Vieweg, Wiesbaden, Germany, 1998, pp. 71–88.

[66] Kulfan, B., "Recent Extensions and Applications of the CST Universal Parametric Geometry Representation Method," 7th AIAA/ATIO Conference, Washington, DC, AIAA Paper 2007-7709, Sept. 2007.

[67] Padulo, M., Maginot, J., Guenov, M. D., and Holden, C., "Airfoil Design Under Geometric Uncertainty with Robust Geometric Parameterization," 11th AIAA Non-Deterministic Approaches Conference, Palm Springs, CA, AIAA Paper 2009-2270, May 2009.

[68] "VGK Method for Two-Dimensional Aerofoil Sections. Part 1: Principles and Results," ESDU, Item 96028, London, April 2004.

[69] Keane, A. J., and Nair, P. B., *Computational Approaches for Aerospace Design: The Pursuit of Excellence*, Wiley, New York, 2005.

[70] "VGK Method for Two-Dimensional Aerofoil Sections. Part 2: User Manual," ESDU, Item 96029, London, Oct. 1996.

[71] Maginot, J., "Sensitivity Analysis for Multidisciplinary Design Optimisation," Ph.D. Thesis, Cranfield Univ., Cranfield, England, U.K., 2007.

[72] "MATLAB Optimization Toolbox 3.1.2. User Guide," MathWorks, Natick, MA, Sept. 2007.

[73] Brass, H., Fischer, J. W., and Petras, K., "The Gaussian Quadrature Method," *Abhandlungen der Braunschweigischen Wissenschaftlichen Gesellschaft*, Vol. 47, 1997, pp. 115–150.

T. Zang
Associate Editor